INFORMATION TO USERS

This manuscript has been reproduced from the microfilm master. UMI films the text directly from the original or copy submitted. Thus, some thesis and dissertation copies are in typewriter face, while others may be from any type of computer printer.

The quality of this reproduction is dependent upon the quality of the copy submitted. Broken or indistinct print, colored or poor quality illustrations and photographs, print bleedthrough, substandard margins, and improper alignment can adversely affect reproduction.

In the unlikely event that the author did not send UMI a complete manuscript and there are missing pages, these will be noted. Also, if unauthorized copyright material had to be removed, a note will indicate the deletion.

Oversize materials (e.g., maps, drawings, charts) are reproduced by sectioning the original, beginning at the upper left-hand corner and continuing from left to right in equal sections with small overlaps.

Photographs included in the original manuscript have been reproduced xerographically in this copy. Higher quality 6" x 9" black and white photographic prints are available for any photographs or illustrations appearing in this copy for an additional charge. Contact UMI directly to order.

Bell & Howell Information and Learning
300 North Zeeb Road, Ann Arbor, MI 48106-1346 USA
800-521-0600

UMI®

COPOLYMERIZATION STUDIES OF TRIOXANE AND DIOXOLANE

by

Mark D. Werner

A dissertation submitted to the Graduate Faculty in Chemistry in partial fulfillment of the requirements for the degree of Philosophy, The City University of New York.

1996

This manuscript has been read and accepted for the Graduate Faculty in Chemistry in satisfaction of the dissertation requirement for the degree of Doctor of Philosophy.

9/16/96
date

Chairman of Examining Committee

9/19/96
date

Executive Officer

Supervisory Committee

The City University of New York

Abstract

Copolymerization Studies of Trioxane and Dioxolane

by

Mark Werner

Adviser : Professor Nan Loh Yang

Polyacetal copolymers are technically important engineering plastics which are competitive with metals, ceramics and nylons in many applications. They are also of fundamental interest since they are the simplest form of polymers with heteroatom backbone . This work focuses on clarifying some of the fundamental processes which occur during this important copolymerization.

The work is divided into three sections. The first section fully details the NMR experiments that were used to objectively assign the main chain pentads and endgroups. The microstructure of the ethylhydroxy, formate and methoxy endgroups were established.

In the second section NMR assignments made in section one are used to follow the copolymerization *in situ* through the "precloud period". The pentad profiles demonstrate that transacetalization does not significantly redistribute ethylene oxide units during this period. Experiments using ^{13}C enriched dioxolane

helped shed light on the facile exchange of methylene oxide units which occurs throughout the "precloud period".

The third section reports the copolymerization of trioxane with 1,5,7,11-tetraoxaspiro[5,5]undecane. This copolymerization has not been reported previously and introduces a carbonate unit into the copolymer backbone. The copolymer was found to have improved thermal stability relative to trioxane-dioxolane copolymer.

Acknowledgments

I would like to extend a very special and sincere thanks to Dr. Nan Loh Yang for his guidance, wisdom and friendship during the course of my studies. He played an integral role in my educational development and provided a wealth of knowledge and encouragement as I strove to achieve my goal and obtain my degree. Thank you Dr. Yang. I will miss you and think of you often as I embark on my career.

The support of the Chemistry Department, College of Staten Island, CUNY and Hoechst Celanese Corporation is gratefully acknowledged.

I would also like to thank all of the faculty members, especially Dr. Odian and Dr. Stark for their friendship and support.

Last, but not least, I would like to thank my loving wife for her support and patience throughout my endeavors

Thank you again, one and all.

TABLE OF CONTENTS

List of Tables

List of Figures

1. BACKGROUND SURVEY

Polyacetals are important engineering plastics which compete with metals, ceramics and nylons in many applications. There are two types of polymers that fall into this category. One is acetal homopolymer that is completely characterized by the oxymethylene, $(CH_2O)_n$,, repeat unit and is better described by the name polyoxymethylene. The other is the acetal copolymer, which has the same polyoxymethylene structure as the homopolymer but its backbone structure is occasionally interrupted by a comonomer unit. In 1990 the combined production capacity of homopolymer and copolymer was 482,000 tons world wide[1]. In addition to their obvious economic importance these polymers are of fundamental interest since they represent the simplest form of macromolecules with heteroatom backbone .

Acetal copolymers were first observed in 1859 by Butlerov[2]. Yet, they were not studied in depth until Staudinger investigated them in the 1920's[3]. In fact, Staudinger's investigations of formaldehyde polymers contributed to the foundations of macromolecular chemistry[4]. Following World War II, studies on polyoxymethylene were continued in industry and at universities throughout the world. However, acetal polymers of sufficient molecular weight to be commercially useful were not prepared until the late 1950's, when Dupont began production of Delrin. Delrin was synthesized by anionic polymerization of highly

pure formaldehyde. The polymer was stabilized by esterifying the inherently unstable hemiacetal endgroups (-O-CH_2OH) with acetic anhydride to yield an acetate end-capped homopolymer[5]. Shortly thereafter, Celanese developed Celcon, a thermally stable copolymer[6] of trioxane and ethylene oxide. Since then, production of acetal resins has rapidly expanded and today they are widely used as replacements for metals in such areas as machinery, appliances, hardware and plumbing. A detailed review of polyacetal history is given by Dolce and McAndrew[7].

After initiation, trioxane homopolymerization begins following a relatively brief "induction period", during which time the concentration of monomeric formaldehyde reaches an equilibrium. The end of the "induction period" is marked by the onset of polymer precipitation from the polymerization solution. Acetal copolymer is commonly produced by the cationic ring-opening copolymerization of trioxane and a cyclic comonomer such as ethylene oxide or 1,3-dioxolane.

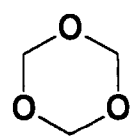

1,3,5-Trioxane

Ethylene Oxide

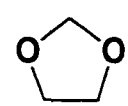

1,3-Dioxolane

Experimentally it was found that during trioxane copolymerization, the "induction period" is extended to varying degrees depending on the comonomer species and its concentration.

Weissermel *et al.*[8,9] reported that when trioxane and ethylene oxide are copolymerized the "induction period" is lengthened substantially. During this period, ethylene oxide is converted to linear low molecular weight copolymer and cyclic oligomers such as 1,3-dioxolane and 1,3,5-trioxepane. Only following the complete consumption of ethylene oxide does solid polymer begin to precipitate.[10,11] The selectivity of the reaction can be explained by the higher basicity of ethylene oxide (pK_b=7.3) relative to trioxane (pK_b=10), as well as by the high degee of ring strain present in the three-membered ethylene oxide ring.

Weissermel *et al.*[12] and Collins *et al.*[13] proposed that dioxolane and trioxepane are formed by an insertion of formaldehyde into ethylene oxide. In this mechanism a small amount of trioxane is decomposed to form formaldehyde. The formaldehyde then reacts with ethylene oxide to yield dioxolane which in turn can react with another formaldehyde to form trioxepane. These two cyclic acetals then copolymerize with trioxane.

More recently Masamoto *et al.*[14] proposed a second mechanism which involves the existence of two previously unreported intermediates, 1,3,5,7-tetraoxacyclononane (TOCN) and 1,3,4,7,10-pentaoxacyclododecane (POCD). In this mechanism trioxane and ethylene oxide react in a one to one molar ratio to

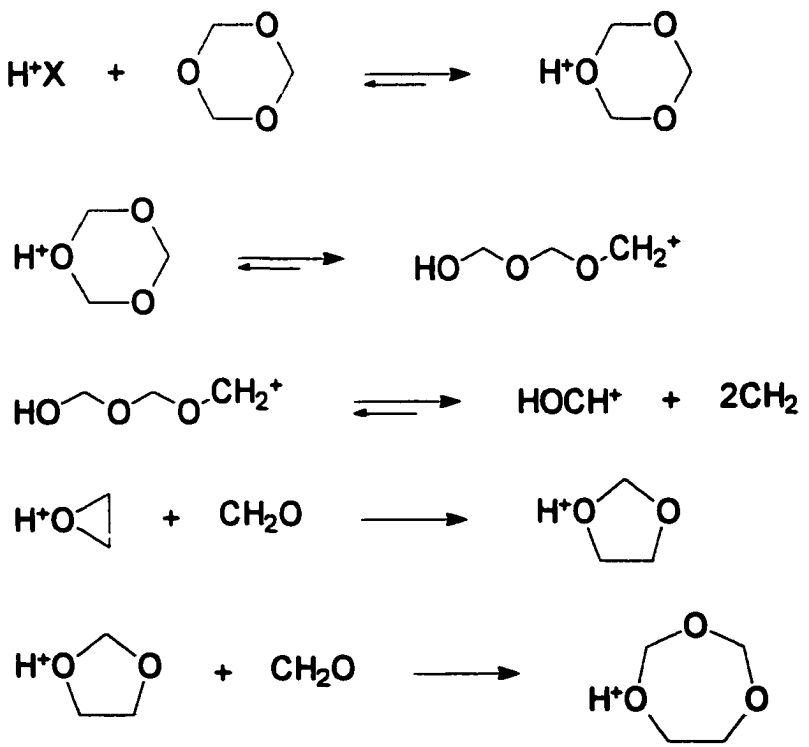

yield TOCN, a nine-membered ring, and in a one to two molar ratio to yield POCD, a twelve- membered ring. These rings then decompose to yield dioxolane and trioxepane. Regardless of how dioxolane and trioxepane rings are formed, it is clear that they are also consumed at a much higher rate than trioxane during the induction period[15].

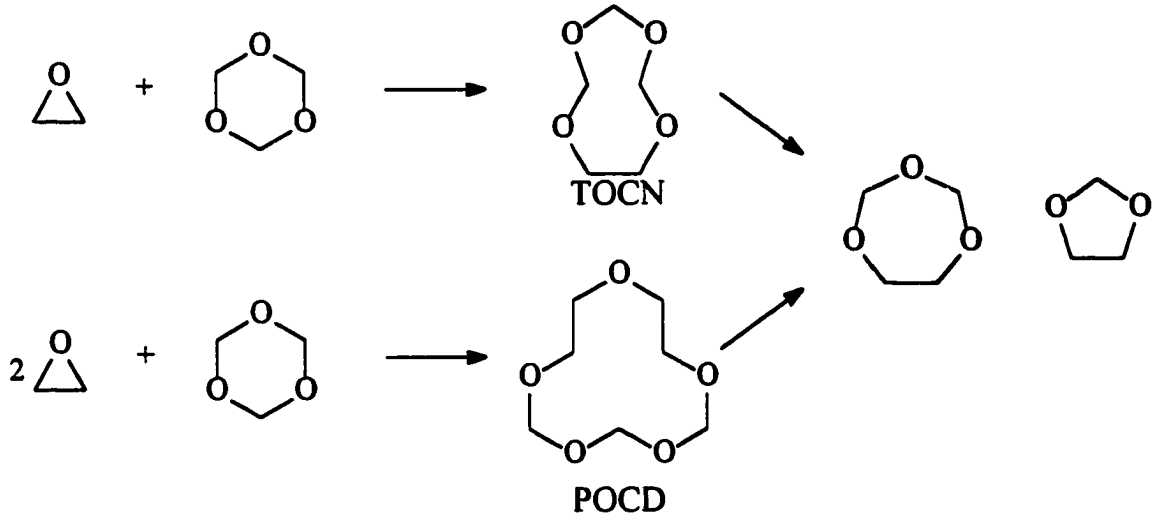

When the comonomer is dioxolane the induction period is also extended relative to that seen in trioxane homopolymerization. Again, it was found that when the polymerization was terminated during the induction period almost all of the dioxolane was incorporated into polymer[16]. Miki *et al.*[17] and Jaacks *et al.*[18] reported the formation of trioxepane as an intermediate in trioxane-dioxolane copolymerization. Miki proposed a backbiting mechanism to explain its formation. In this mechanism the comonomer is first incorporated in a growing polymer chain. Then the active center of the polymer rolls back on itself and

attacks an oxygen in the chain. The result is an intra-chain transfer and formation of a ring.

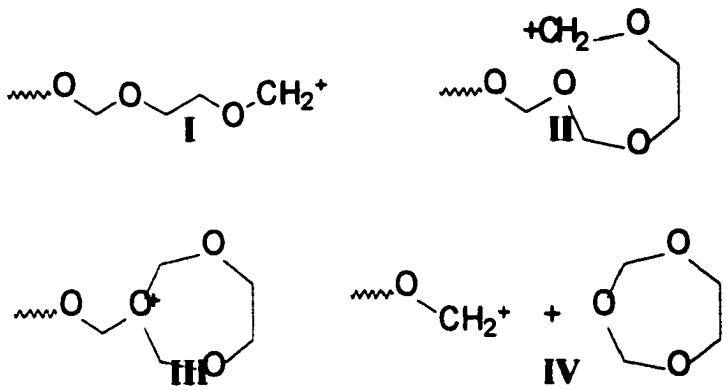

Mengoli *et al.*[19] proposed an insertion mechanism and this was latter supported by Lu *et al*[20]. Lu demonstrated through proton NMR that ring expansion occurs prior to the appearance of linear polymer sequences.

As was seen in ethylene oxide-trioxane copolymerization, dioxolane and trioxapane are preferentially incorporated relative to trioxane during the induction period. This suggests that the resulting copolymer should consist of two types of blocks: one relatively rich in ethylene oxide units and the other of virtually pure polyoxymethylene. It has long been established that this is not the case. Conversely, the ethylene oxide units are found to be distributed almost randomly throughout the polymer chain.

Two theories have been proposed to explain the redistribution. One widely accepted process is chain transfer to polymer or transacetalization[21]. In this scheme the active chain end of the growing polymer attacks the acetal oxygen of another polymer chain, terminating the growing chain and simultaneously starting a new growing chain. This process is thought to occur frequently during the copolymerization because the acetal oxygens in the chain are more

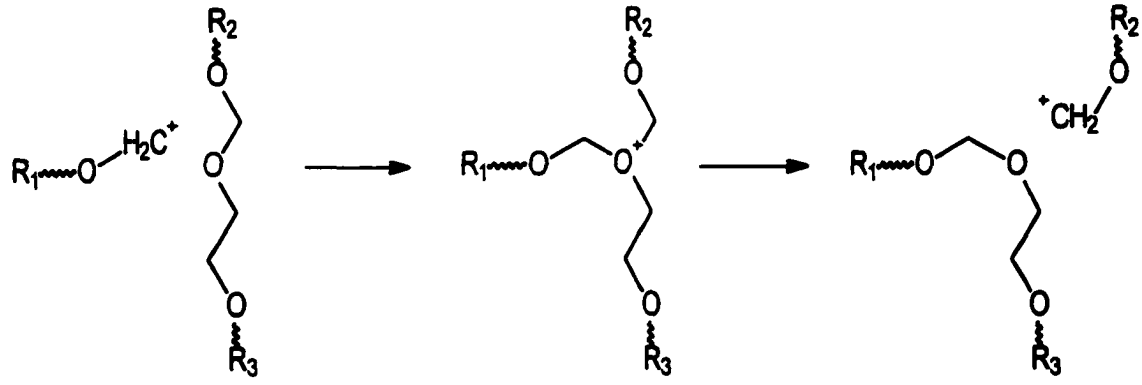

basic than those in trioxane. The second redistribution mechanism is based on the depolymerization of the soluble polymer formed during the induction period[22]. According to this theory, as crystalline polymer starts to form, the soluble polymer degrades, releasing DOL which is then randomly incorporated into the crystalline copolymer.

References

[1] Masamoto, J., Iwaisako, T., Yoshida, K., Matsuzaki, K., Kagawa, K., Nagahara, H. *Makromol. Chem., Macromol. Symp.*, 1991, 42/43, 409

[2] Butlerov, A.M. *Ann.* 1859, **3**, 242

[3] Staudinger, H. *Die Hochmolecularen Organischen Verbingen*, Springer: Berlin, 1932

[4] Kern, W., Cherdron, H., Jaacks, V. Angew. Chem., 1961, **73**, 177

[5] MacDonald, R. N. (to E. I. du Pont de Nemours & Co. Inc.) U. S. Patent 3 027 352, March 27, 1956

[6] Walling, C., Brown, F., Bartz, K. (to Celanese Corp.) U.S. Patent 3 027 352, March 27, 1962

[7] Dolce, T., McAndrew, F. "Acetal Copolymers, A Historical Perspective," in High Performance Polymers : Origins and Development, G. Kirshenbaum and R. Seymor, Eds., American Chemical Society : Washington, D.C., 1986, p 115.

[8] Weissermel, K., Fisher, E., Gutweiler, K. *Kunstoffe*, 1964, **54**, 410

[9] Weissermel, K., Fisher, E., Gutweiler, K., Hermann, H. D., Cherdron, H. *Angew. Chem. Int. Ed.*, 1967, **6**, 526

[10] Chen, C.S.H.; DiEdwardo, A. *Adv. Chem. Ser.*, 1969, **91**, 359.

[11] Chen, C.S.H., DiEdwardo, J. *Macromol. Sci. Chem.*, 1970, **4**, 349.

[12] Weissermel, K., Fisher, E., Gutweiler, K., Hermann, H. D. Cherdron, H., *Angew. Chem. Int. Ed.*, 1967, **6**, 526

[13] Collins, G.L., Greene, R.K., Benardinelli, F.M., Ray, W.H. *J. Polym. Sci. Polym. Chem. Ed.*, 1981, **17**, 667.

[14] Masamoto, J., Iwaisako, T., Yoshida, K., Matsuzaki, K., Kagawa, K., Nagahara, H. *Makromolek. Chem., Macromolec. Sym.*, 1991, **42/43**, 409

[15] Collins, G.L., Greene, R.K., Berardinelli, F.M., Ray, W.H. *J. Polym. Sci. Polym. Chem. Ed.*, 1981, **17**, 667.

[16] Price, M. B., Mcandrew, F. B. *J. Macromolec. Sci., A-I,* 1967, **2**, 231

[17] Miki, T., Higashimura, T., Hayashi, K., Okamura, S. *J. Polym. Sci., Polym. Lett.*, 1967, **5**, 65

[18] Jaacks, V. *Adv. Chem. Ser.*, 1969, **91**, 371

[19] Mengoli, G., Furlanetto, F. *Makromolek. Chem.*, 1975, **176**, 143

[20] Lu, N., Collins, G. L., Yang, N. L. *Macromol. Chem., Macromol. Symp.*, 1991, **42/43**, 425

[21] Wessermel, K., Fisher, E., Gutweiler, K. *Kunstoffe*, 1964, **54**, 410

[22] Jaacks, *op. cit.*,

2. Thesis Statement and Outline

Although polyacetal copolymers represent an important class of high performance plastics today, the copolymerization mechanism involved is still not well-developed and their structures have not been delineated in detail. This thesis reports a fundamental investigation of the copolymerization and the first synthesis of a polyacetal copolymer with a co-unit of high dipole moment.

Prior to the present work, the copolymerization process was observed in two studies using high resolution ^{1}H NMR[1,2]. The studies pointed out that NMR offered the potential ability to simultaneously monitor the concentrations of all species directly *in situ*. However, the first study drew conclusions on the polymerization mechanism based on erroneous chemical shift assignments, and the second study failed to resolve all of the components present in the system due to overlapping resonances. In this dissertation, high field ^{13}C NMR in conjunction with isotope labeling of comonomers and copolymerization with model comonomers was employed to examine the copolymerization process in further detail.

Since our study of the copolymerization process depends heavily on NMR spectroscopy, section III-A describes the assignment process which was used to firmly establish the identity of each resonance in the ^{1}H and ^{13}C NMR spectra. It describes in detail the use of conventional one-dimensional and two-dimensional

NMR techniques together with several recently developed two-dimensional NMR techniques. The knowledge of polyacetal copolymer microstructure has been limited to pentad sequences and some endgroups at a rudimentary level. This work extends our understanding to heptads and sequence structure of endgroups. It also demonstrates the great potential that modern high field NMR spectroscopy has to offer to polymer chemistry.

Section III-B uses the ^{13}C NMR assignments that were established in III-A to follow the polymerization kinetics. By carefully controlling the concentration of the comonomers and water in the bulk we were able to control the rate of polymerization. This allowed us to accurately monitor the concentrations all of the chemical species present during the polymerization.

Finally, in section III-C, trioxane was copolymerized with 1,5,7,11-tetraoxaspiro[5,5]undecane (SOC). SOC like DOL is more reactive than TOX and these two copolymerizations proceed in a similar manner. However once SOC polymerizes the polymer can not degrade to yield SOC. This means that SOC does not participate in the complex equilibrium that controls TOX -DOL copolymerization and as such it should help to clarify the role that the equilibrium plays. The resulting TOX-SOC copolymer has not previously been synthesized nor has an acetal copolymer which contains a carbonate linkage in the backbone.

References

[1] Chen, C. S. H., Di Edwardo, A. *Adv. in Chem.*,1969, **91**, 359

[2] Lu, N., Collins, G. L., Yang, N. L. *Macromol. Chem., Macromol. Symp.*, 1991, **42/43**, 425

3. RESULTS AND DISCUSSION

A) SEQUENCE and ENDGROUPS

The main chain sequence distributions of the methylene oxide (M)and ethylene oxide (E) units in copolymers of 1,3-dioxolane (DOL) and 1, 3, 5 - trioxane (TOX) have been the subject of two previous studies[1,2]. The first study identified three M-centered triad sequences (EME, MME and MMM) and one resonance for all E-centered sequences in 60 MHz proton NMR spectra. The resonances were assigned by varying the feed ratio of the monomers and by comparison with model compounds. The second study used shift reagents to identify six methylene oxide centered pentad sequences and two ethylene oxide centered pentads in 25.2 MHz ^{13}C NMR spectra. The MMMMM pentad resonance was assigned by comparison with the spectra of TOX homopolymer and the MEMEM pentad resonance was assigned by comparison with the spectrum DOL homopolymer. The remainder of the resonances were assigned by varying feed ratios and through statistical methods.

Although these studies made important contributions toward understanding the microstructure of TOX-DOL copolymer, recent advances in NMR spectroscopy have made it possible to determine connectivities between neighboring monomer units even when they are bridged by a heteroatom[3,4]. By applying these techniques to TOX-DOL copolymer we have been able to

objectively assign both the proton and the carbon spectra. The following two-dimensional experiments were used:

* PFG-HMQC(pulsed-field-gradient heteronuclear multiple-quantum correlation)
* PFG-HMBC(pulsed-field-gradient heteronuclear multiple-bond correlation)
* HMQCTOCSY(heteronuclear multiple-quantum correlation total correlation spectroscopy)

Recently, gradient experiments have been used to identify structural units which join polyisobutylene (PIB) and polybutadiene (PBD) blocks in synthetic PIB-b-PBD[5]. The work showed that NMR was capable of detecting units present at the low concentration level of 1 part in 10^{-4}-10^{5} relative to the repeat units of the main chain. Pulsed field gradients (PFG) allow the selection of desired signals without phase cycling. This is a critical advantage when the desired signals are small and undesired signals are large, as is the case in HMBC experiments. In conventional phase cycled experiments imperfect cancellation of undesired signals results in t_1-noise ridges. These ridges can severely interfere with the observation of weak signals (e.g.end groups, junction units). The excellent sensitivity of PFG experiments has also made it possible for us to complete our assignment of the

copolymer microstructure by identifying the resonances of the end groups which arise from the copolymerization of trioxane and dioxolane.

Our assignment process was started by establishing heteronuclear single

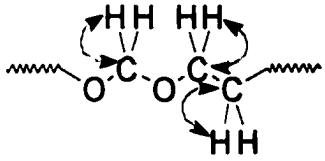

bond ^{1}H-^{13}C correlations with the PFG-HMQC experiment. Based on information available from one-dimensional ^{1}H and ^{13}C spectra tentative assignments for as many resonances as possible were made. This was followed by a PFG-HMBC experiment which provides multiple bond ^{1}H-^{13}C correlations.

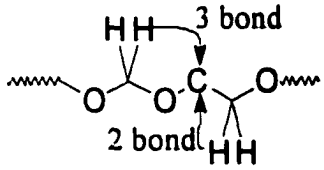

Through comparisons of the single bond correlations (PFG-HMQC) and the multiple bond correlations (PFG-HMBC) we were able to determine which structural units are attatched to each other in the main chain sequences of the polymer. However, PFG-HMBC correlations result from J coupling and are

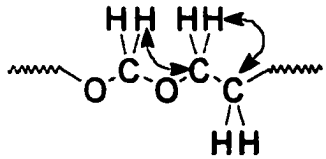

dependent only on the strength of the coupling and the spin-spin relaxation time. The experiment cannot distinguish between two bond and three bond correlations. Making this distinction in the case of end groups that possess both methylene oxide and ethylene oxide units is critical since the ethylene oxide unit can show correlations to itself and to an adjoining methylene oxide. We make this critical distinction using the HMQCTOCSY experiment. In this experiment protons which

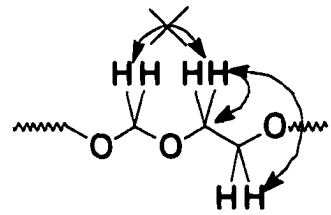

are part of the same spin system(not separated by a heteroatom) are correlated to each other and to the carbons they are directly bonded to. The experiment is especially valuable in the TOX-DOL copolymer system since any resonance which shows TOCSY cross peaks must come from an ethylene oxide unit. This immediately distinguishes PFG-HMBC resonances resulting from inter-unit 3 bond correlations from those due to intra-unit 2 bond correlations. We were able to develop a detailed structure of the copolymer using a combination of these three two-dimensional experiments performed on samples of relatively low molecular weight.

EXPERIMENTAL

COPOLYMER SYNTHESIS

The copolymer samples were prepared using a procedure as follows. Trioxane (5.92g ,0.197mol) and DOL (3.35g ,0.045 mol) were placed in a dry reaction tube containing a magnetic stir bar. The tube was sealed with a septum and placed in a 70 °C oil bath. After approximately 15 minutes, 10 ul ($48x10^{-6}$ mol) of BF_3OBu_2 was injected into the comonomer solution. The reaction was carried out overnight at 70 °C. The resulting copolymer was pulverized. and the powder was stirred in 50 ml of methanol containing 1% triethyl amine to destroy any remaining initiator. The methanol and remaining TOX or DOL were removed by placing the mixture under vacuum at 40 °C for 4 hours.

NMR EXPERIMENTS

Copolymer samples (100 mg) were dissolved by gently heating in 1.0 ml a solution of ca 20% v/v 1,1,1,3,3,3-hexafluoro-2-propanol in $CDCl_3$. The resulting solution was filtered through glass wool directly into a 5mm tube to remove any insoluble copolymer. All experiments were carried out at 40 °C on a Varian Unity Plus Spectrometer operating at a ^{1}H resonance frequency of 599.95 MHz and a ^{13}C resonance frequency of 150.868 MHz.

PFG-HMQC EXPERMENT

The PFG-HMQC spectrum was recorded using the pulse sequence of Hurd *et al.*[6] with a 0.641 second acquisition time. The relaxation delay between scans was 0.935 sec and the delay for polarization transfer was set for a J(C,H) of 155 Hz. WURST decoupling was used in the carbon channel during acquisition. The specta were acquired over an F_2 spectral window of 1547.9 Hz and an F_1 spectral window of 10259 Hz. The number of transients was 16 per increment and 450 time increments were collected using the magnitude mode. Ninety degree pulse widths were 11.1 and 16.0 μs for ^1H and ^{13}C, respectively. Gradient pulses were 0.2 ms in duration and were about 20, 20 and 10 G/cm for the first, second and third pulses, respectively. The total accumulation time was 3 hrs and 48 min. The specta were processed using Varian VNMR software. The F_1 dimension was forward extended to 1K by linear prediction and then zero filled to 4K (2.50 Hz/pt); the F_2 dimension was zero filled to 4K (0.39 Hz/pt). A 90° shifted sine-bell apodization function was applied in both domains prior to Fourier transformation.

PFG-HMBC EXPERIMENT

The PFG-HMBC spectrum was recorded using the pulse sequence of Rinaldi *et al.*[7] with a 0.641 second acquisition time and a 0.935 second relaxation delay between scans. The pulse widths, spectral windows and number of time

increments were identical to those used in the PFG-HMQC. The number of transients was 32 per increment. For the first delay, a value of 3.2ms $\left(\frac{1}{2^1 J(CH)}\right)$ was used to suppress the one bond CH coupling. Theoretically, the second delay should be set to $\left(\frac{1}{2^n J(CH)}\right)$, however the 3 bond coupling across the oxgen is only about 5 Hz and would result in the delay being 100 ms. To avoid the decay of ^{1}H magnetization that would occur during such a lengthy delay the second delay was set to 0.45 ms. The total acquisition time was 7hrs and 32min. The spectra were processed in an identical manner to that used for the PFG-HMBC.

HMQC-TOCSY

The HMQC-TOCSY was recorded using the pulse sequence of Lerner *et. al.*[8] and acquired by the hypercomplex method[9]. The acquisition time was 0.170 sec and the relaxation delay was 1.5 sec. The 90° pulse widths were 11.1 and 16.0 μs for ^{1}H and ^{13}C, respectively. The delay for polarization transfer was set for ^{1}J(CH) of 160 Hz and the delay after the BIRD portion of the sequence was set for 700 ms. The spinlock mixing time was 40 ms using the clean TOCSY pulse sequence of Griesinger et al.[10]. The 90° pulse during spinlock was 20μs and the window was 40μs. GARP-1 decoupling was used on the carbon channel during acquisition. The spectra were acquired over an F_2 spectral window of 6022.3 Hz and an F_1

spectral window of 18107 Hz. The number of transients was 16 per increment and 512 time increments were collected. The spectra were processed using Varian VNMR software. The F_1 dimension was forward extended to 1K by linear prediction and then zero filled to 4K(4.42 Hz/pt); the,F_2 dimension was zero filled to 2K (2.94 Hz/pt).

POLYMER MAIN CHAIN

Figure III A-1 represents a ^{13}C NMR spectrum of the copolymer. The top section shows the upfield region which contains the sequence peaks from ethylene oxide units and several end groups. The bottom section shows the downfield region which contains the sequence peaks from methylene oxide units. As shown in the Table 1, six M-centered pentads and three E-centered pentads are possible in the copolymer. The number of pentads observed is limited to nine because E units cannot form contiguous to each other. For two E units to become bonded, a highly unstable carbenium ion would have to exist on the ethylene unit during the copolymerization process. This is highly unlikely since the carbenium on the methylene unit is stabilized by the α oxygen and is greatly preferred.

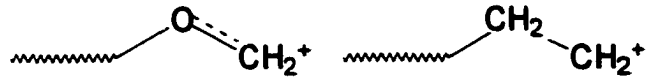

The spectrum shows the resonaces from the six M-centered pentads and two resonances from the three E-centered pentads. The Upfield E-centered resonance contains both the EMEMM and EMEME pentads while the downfield E

Table 1. Pentad sequences possible in copolymer microstructre

M centered pentads	E centered pentads
MEMEM	MMEMM
MMMEM=MEMMM	EMEME
MEMME=EMMEM	EMEMM=MMEME
MMMMM	
EMMMM=MMMME	
EMMME	

centered resonance is solely from the MMEMM pentad. The ^{1}H spectrum (Figure III A-2) shows resonances from three methylene centered pentads and two E centered triads. The microstructure of the main chain was established by first determining which pentad sequences should have multiple bond correlations to each other. Each pentad has to have correlation to two flanking pentads. For

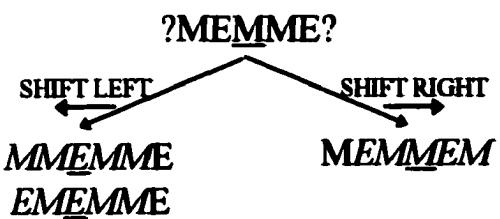

example the MEMME sequence should show correlations to the M centered sequence that is shifted one unit to the right (EMMEM) and to the two E centered sequences, EMEMM and MMEMM, that are shifted one unit to the left. Table 2. lists expected multiple bond correlations and the correlations observed in the HMBC spectrum (Figure III A-3) for the main chain pentad sequences. (also see figure III A-7)

Table 2. Predicted and observed multiple bond correlations.

	PENTAD	Correlations expected	Observed correlations
1	**MEMEM**	EMEMM, EMEME	EMEMM, EMEME
2	**MMMEM=MEMMM**	MMEMM, EMEMM EMMME, MMMME	MMEMM EMMME, MMMME
3	**MEMME=EMMEM**	MMEMM, EMEMM EMMEM	MMEMM EMMEM
4	**MMMMM**	EMMMM, MMMMM	EMMMM, MMMMM
5	**EMMMM=MMMME**	MEMMM, MMMMM EMMMM	EMMMM, MMMMM MEMMM
6	**EMMME**	MEMMM	MEMMM
7	**MMEMM**	MMMEM, EMMEM	MMMEM, EMMEM
8	**EMEME**	MEMEM	MEMEM
9	**EMEMM=MMEME**	MEMEM, MEMME MEMMM	MEMEM, MEMME MEMMM

ENDGROUP ASSIGNMENTS

The copolymer endgroups were identified many years ago by Jaacks[11] using chemical means. They include four distinct chemical groups:

* Hemiacetal, which is unstable and depolymerizes to liberate formaldehyde under mild conditions;
* Formate, which is moderately stable and decomposes at elevated temperatures also liberating formaldehyde;
* Methoxy which is stable
* Ethylhydroxyl which is stable.

Although the existence of these endgroups has been established they have never been completely resolved and identified by NMR. Since NMR data can give detailed quantitative structural information it is important that the resonances for each endgroup be determined.

Using a Varian Unity Plus NMR operating at a ^1H resonance frequency of 600 MHz to analyze a low molecular weight copolymer sample($M_n \approx 10000$), we assigned all but the hemiacetal end group. The failure to identify this group can be accounted for by its instability. It is likely that the groups are destroyed during the dissolution process when the polymer is gently heated. This process is analogous to the one described earlier which is used to remove the same

endgroups thermally. The result of this degradation process is the conversion of the hemiacetal chain ends to ethylhydroxyl chain ends.

The methoxy endgroups show two distinct resonances at 55.30, 3.39 ppm and 55.86, 3.41 ppm in the HMQC spectrum (Figure III A-4). The resonance at 55.86 ppm shows further splitting in the 1D ^{13}C spectrum, but is not resolved in the two dimensional spectrum. These multiple resonances are the result of microstructure differences in the chain as shown in Figure III A-5. The methoxy at 55.30 ppm ($\underline{C}H_3OME$)shows correlations in the HMBC spectrum (Figure III A-6) to protons in the methylene oxide region at 4.64 ppm. These protons are attached to a carbon at 96.45 ppm and show an additional correlation in the HMBC spectrum to a carbon in the ethylene oxide region at 67.05 ppm. The methoxy resonance at 55.86 ppm (CH_3OMM) is only slightly split because these methoxy units (CH_3OMMM & CH_3OMME) have almost the same microstructure, i.e. both are attached to two consecutive M units. The difference is due to the third unit, in one case an E unit and in the other an M unit. This can be seen in the PFG-HMBC spectrum (Figure III A-3) where the methoxy protons (3.41ppm) have correlations to two carbons in the methylene oxide region (93.97, 93.62 ppm). The carbon at 93.62 ppm has a long range correlation (Figure III A-7) to protons in the methylene oxide region that are adjacent to an ethylene oxide

unit. The carbon at 93.97 is also correlated to protons in the methylene oxide region, that are adjacent to protons in the MMMMM pentad.

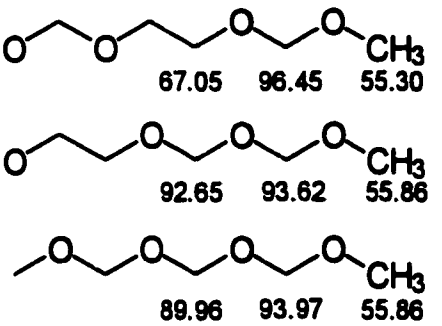

Figure III A-5. ^{13}C NMR assignments of methoxy endgroups.

The formate endgroups are identified starting from the formate proton which has a broad resonance at 8.03 ppm. This proton has long range correlations to two carbon resonances (63.35, 64.42ppm) in the ethylene oxide region (Figure III A-8). Both of these carbons show **HMQCTOCSY** cross peaks, the upfield peak to 65.60ppm and the downfield peak to 66.14 ppm (Figure III A-9). The peak at 65.60 shows an HMBC crosspeak to methylene oxide protons at 4.74 ppm,

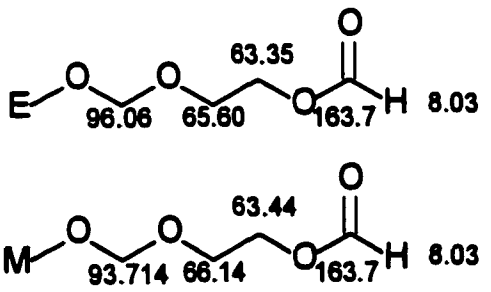

Figure III A-11. ^{13}C NMR assignments of formate endgroups

which are attached to an ethylene oxide unit (Figure III A-10). The peak at 66.14 ppm has a cross peak to methylene oxide protons at 4.83 ppm, which are attached to another methylene oxide unit.

The third endgroup identified was ethylhydroxyl. The carbon directly connected to the hydroxy group ($HOCH_2$ CH_2M) shows two signals (62.03, 62.19 ppm) due again to microstructure differences. Both of the signals have HMBC cross peaks to protons at 3.72 ppm. **HMQCTOCSY (Figure III A-9)**

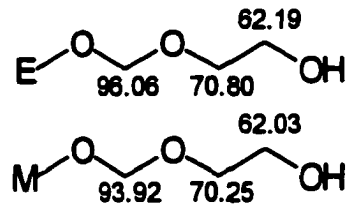

Figure III A-12. ^{13}C NMR assignments of ethylhydroxyl endgroups

resonances establishes the correlation of the upfield ^{13}C signal ($HOCH_2CH_2MM$; 60.03 ppm) to the carbon of the same E unit ($HOCH_2$ CH_2MM) at 70.25 ppm and the downfield ^{13}C singlet ($HOCH_2$ CH_2ME; 62.19 ppm) to the carbon of the same E unit ($HOCH_2$ CH_2ME)at 70.80 ppm. The carbon at 70.25 has an HMBC cross peak to methylene oxide protons in the MME triad. The carbon at 70.80 has an HMBC cross peak to methylene oxide protons in the EME triad.

References

[1] Yamahita, Y., Asakura, T., Okada, M., Ito, K. *Makromol. Chem.*, 1969, **129**, 1

[2] Fleischer, D., Schulz, R. C. *Makromol. Chem.*, 1975, **176**, 677

[3] Beshah, K. *Makromol. Chem.*, 1993, **194**, 3311

[4] Beshah, K. *Macromol. Symp.*, 1994, **86**, 34

[5] Rinaldi, P. L., Keifer, P. A. *J. Magn. Reson.*, 1994, **108**, 259

[6] Hurd, R. E., John, B. K. *J. Magn. Reson.*, 1991, **91**, 648

[7] Rinaldi, *op. cit.*,

[8] Lerner, L., Bax, A. *J. Magn. Reson.*, 1986, **69**, 375

[9] States, D. J., Haberkorn, R. A., Ruben, D. J. *J. Magn. Reson.*, 1982, **48**, 286

[10] Griesinger, C., Otting, G., Wüthrich, K., Ernst, R. R. *J. Am. Chem. Soc.* 1988, **110**, 7870

[11] Jaacks, V., Frank, H., Grünberger, E., Kern, W. *Makromol. Chem.* 1968, **115**, 290

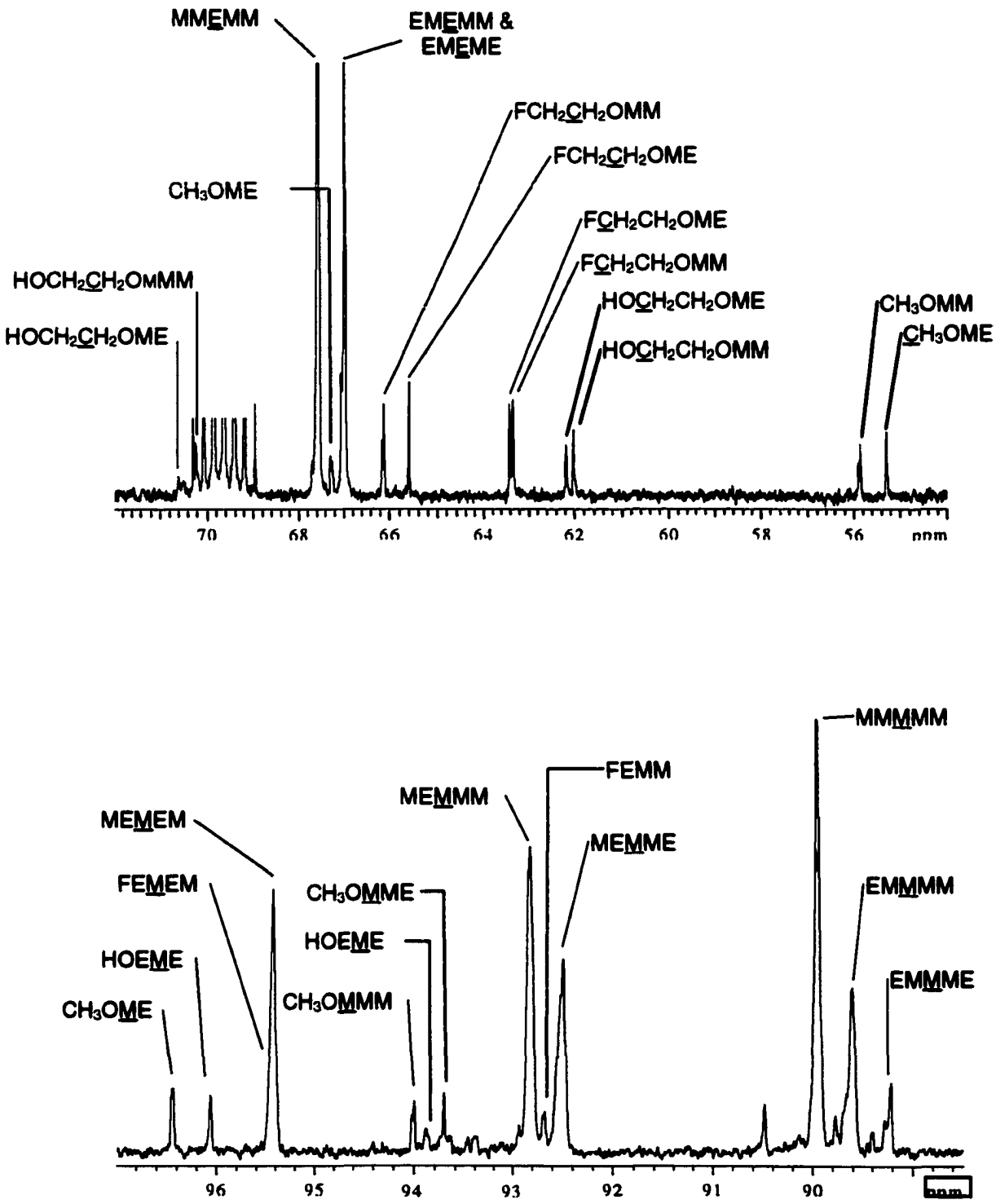

Figure III A-1. 150 MHz Carbon spectrum of TOX DOL copolymer

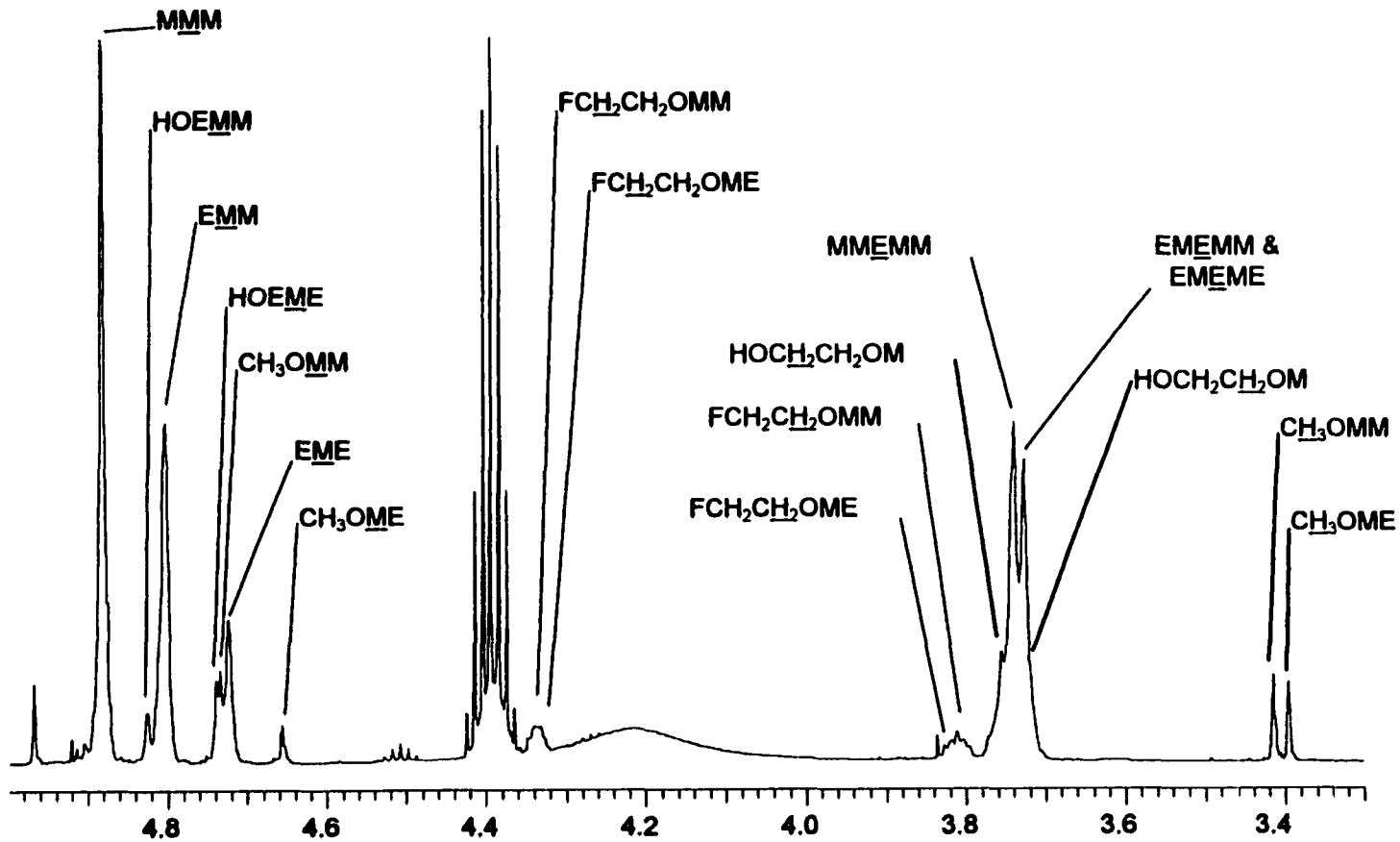

Figure III A-2. 600 MHz Proton spectrum of TOX DOL copolymer. The broad hump in the center of the spectrum is due to polymer which is not fully dissolved.

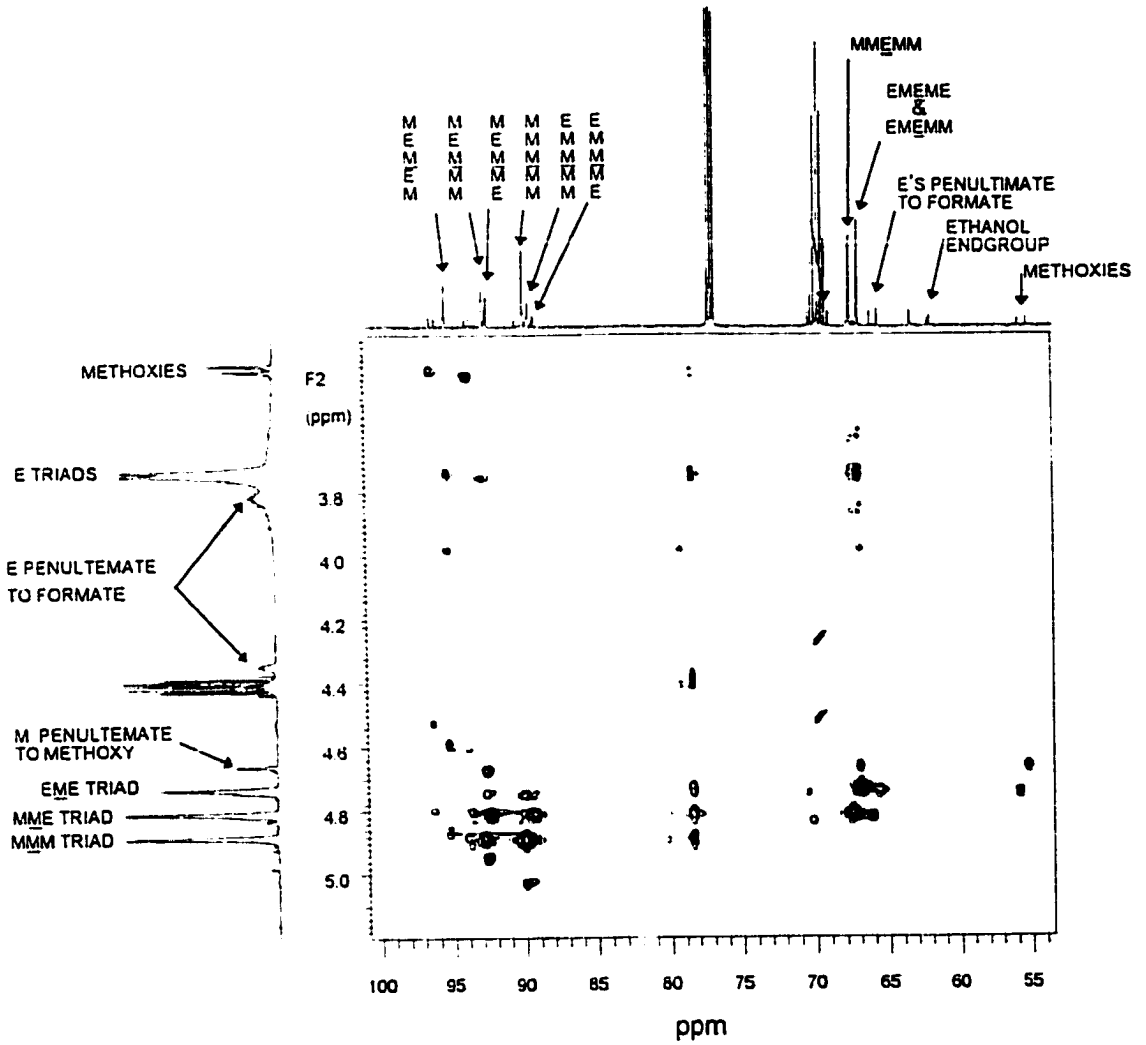

Figure III A-3. GHMBC spectrum of TOX-DOL copolymer

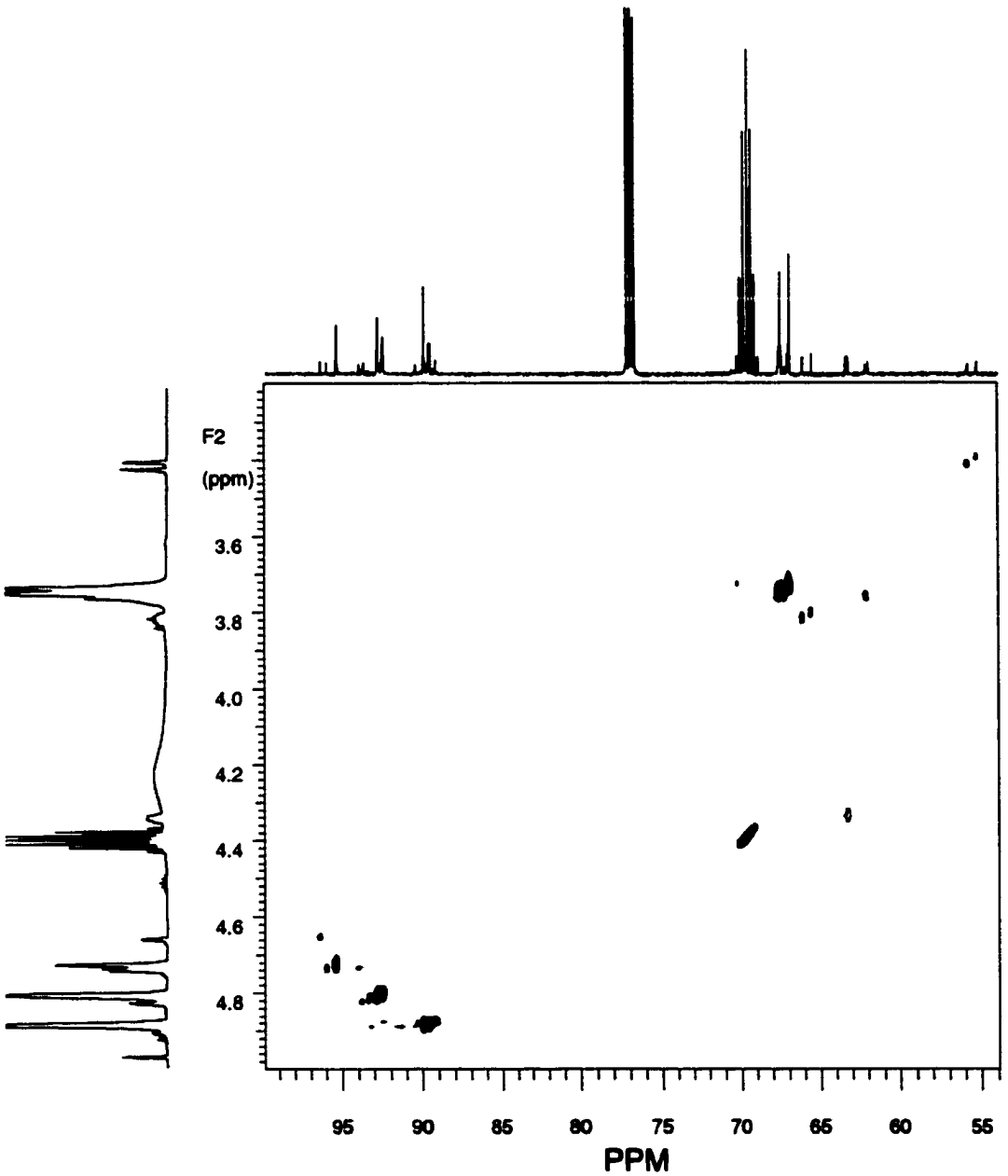

Figure III A-4. HMQC spectrum of TOX-DOL copolymer.

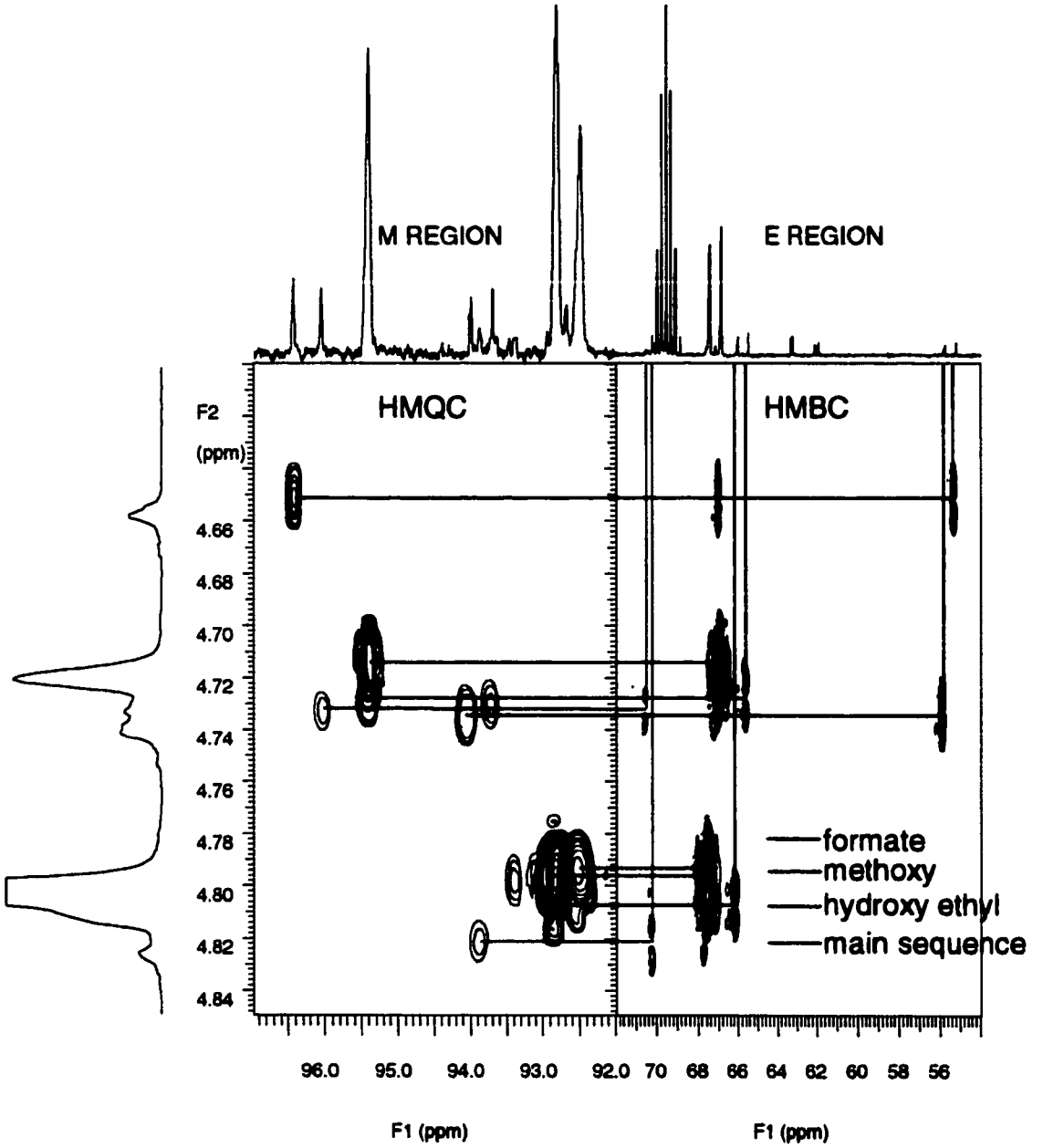

Figure III A-6. Correlations between HMBC (Right) and HMQC (left)

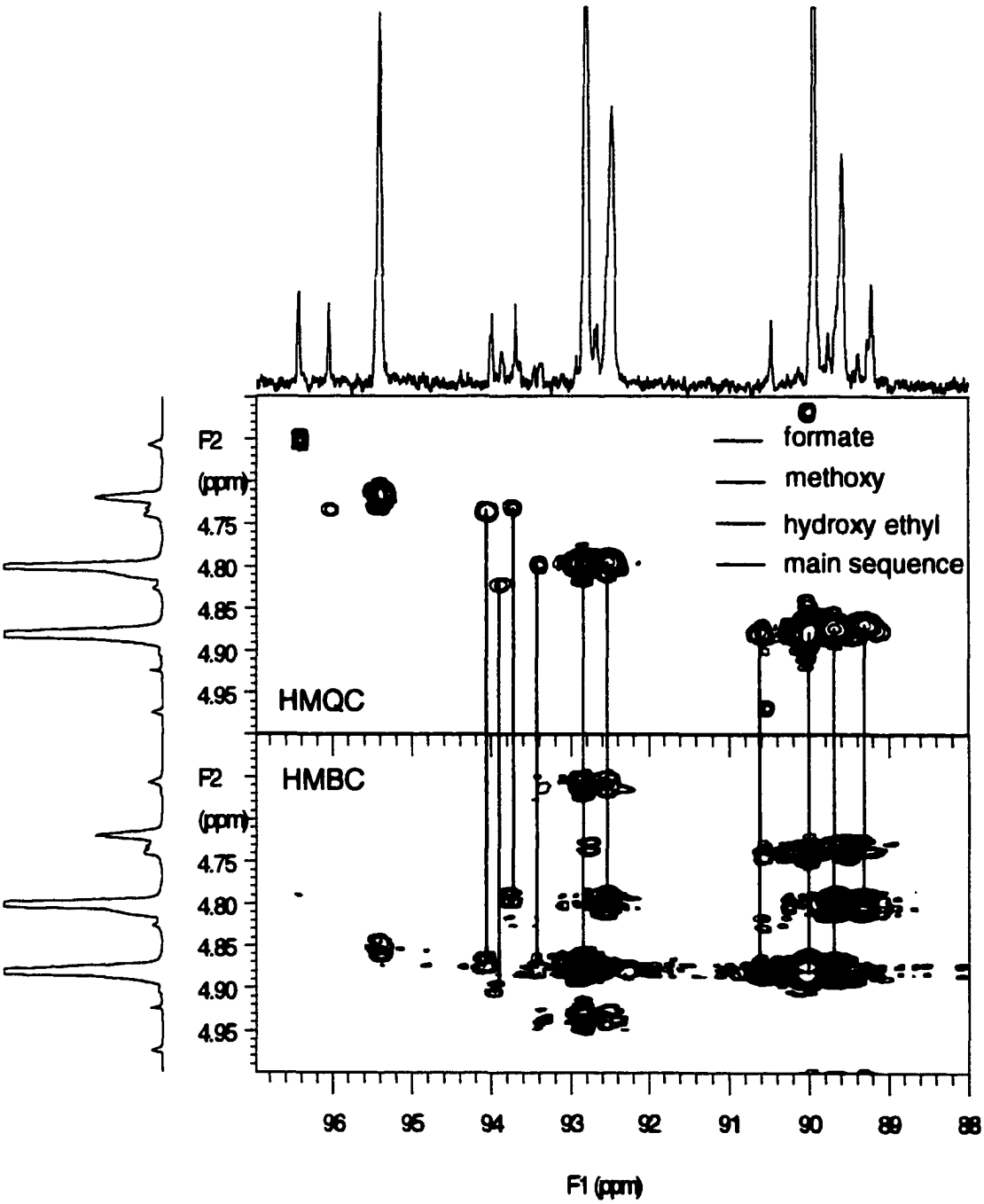

Figure III A-7. Correlations between HMBC (Bottom) and HMQC (TOP)

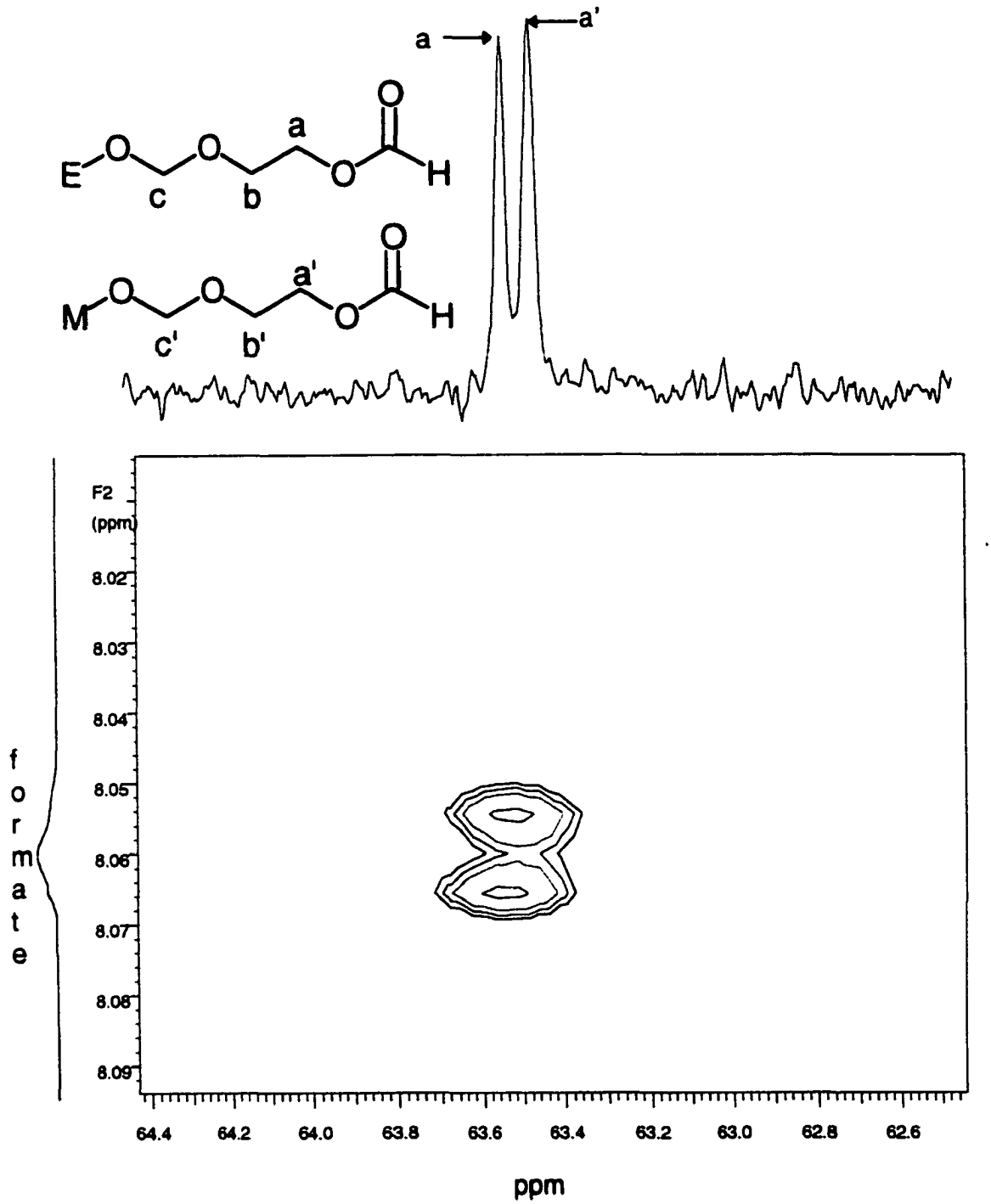

Figure III A-8 GHMBC spectrum of trioxane-dioxolane copolymer showing correlation of the formate protons to adjacent ethylene oxide units

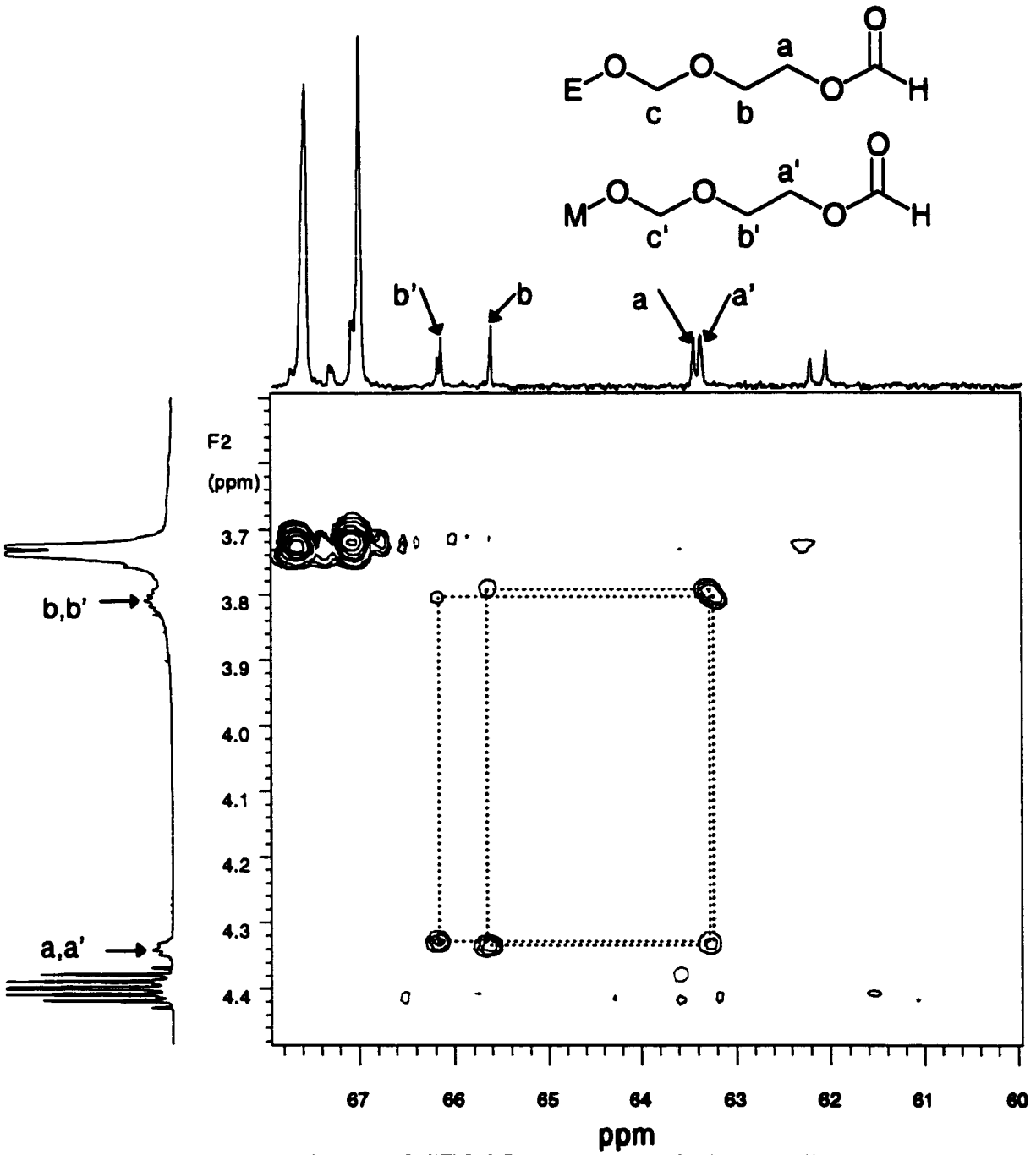

Figure III A-9 HMQCTOCSY spectrum of trioxane-dioxolane copolymer showing correlations of ethylene oxide units adjacent to the formate end group.

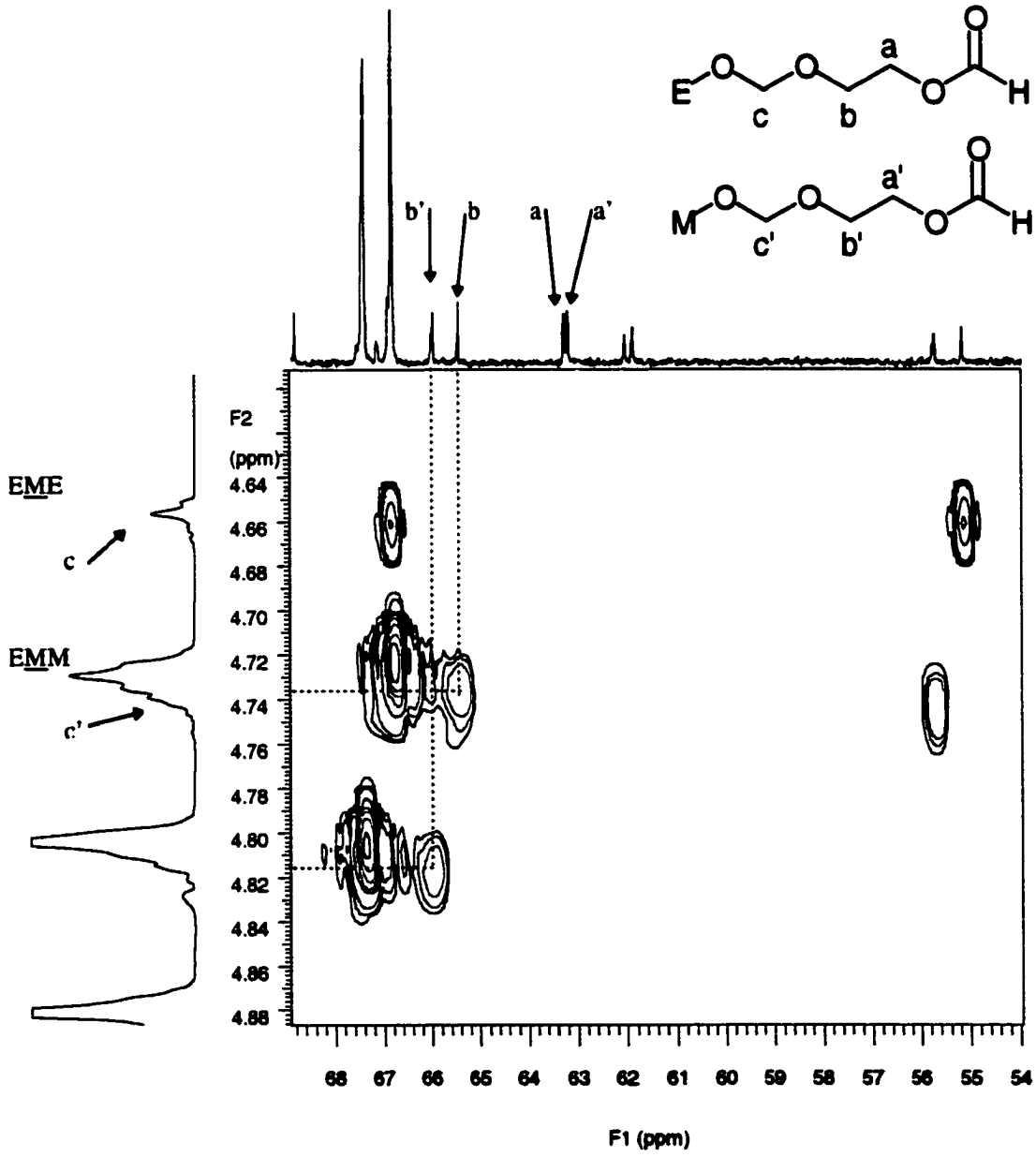

Figure III A-10. GHMBC spectrum of trioxane-dioxolane copolymer showing correlations of ethylene oxide units adjacent to the formate endgroups and methylene oxide triad resonances.

B) TRIOXANE DIOXOLANE COPOLYMERIZATION

Copolymerization of trioxane(TOX) and dioxolane(DOL) has been the subject of intense investigation. Because of the lack of solubility of the copolymer with low dioxolane incorporation, most previous studies focused on the early stages of polymerization at low conversion, or on systems with high dioxolane feeds. Because of the technological importance of TOX-DOL copolymers, it is of great interest to develop a complete description of the process from the beginning to the later stage of copolymerization, particularly when dioxolane incorporation is limited. The objective of our study is to follow the entire course of the cationic bulk copolymerization of (TOX) and (DOL).

As shown by Jaacks[1], DOL is preferentially incorporated into the growing polymer chains during the early stages of the polymerization. This would suggest that the resulting copolymer would consist of two types of blocks, one relatively rich in ethylene oxide units and the other of virtually pure polyoxymethylene. It has long been established that this is not the case. Conversely, in the final products the ethylene oxide units are found to be distributed almost randomly throughout the polymer chain. We have attempted to elucidate the course of the bulk copolymerization using ^{13}C NMR monitoring of various species involved in the reaction. During the period before crystalline polymer begins to precipitate from solution, i.e. the "precloud period", the NMR observation was done *in situ* on the comonomer melt. However, ^{13}C NMR is not suitable for quantifying

resonances for the entire course of polymerization from liquid to solid state due to the large range of molecular motion involved in the system with both states present. Thus, the post cloud point processes could not be observed directly. Instead, the polymerizations were performed and samples were withdrawn and quenched at various times during the post cloud point period. The samples were then dissolved and NMR spectra were acquired.

Experimental

Monomers

Trioxane for these experiments was refluxed continuously over sodium-potassium amalgam, under dry argon, in a Fuchs style reflux apparatus. The still head, shown in Figure III-B 1, was oil jacketed to keep the TOX at 80°C. As needed, it was collected in the storage head where it was removed by hot syringe. DOL was stirred continuously over lithium aluminum hydride, under dry argon in a standard Fuchs reflux apparatus. DOL was refluxed for a minimum of 2 hours before being collected in the storage head where it was removed by hot syringe for immediate use.

DOL monomer with 33% ^{13}C enrichment of the acetal carbon , i.e. C-1, was synthesized from ^{13}C labelled paraformaldehyde and ethylene glycol. Two grams of 99% ^{13}C enriched paraformaldehyde and 4.0 g of non enriched paraformaldehyde were combined in a 100 ml round bottom flask together with 12.9 g (excess) of ethylene glycol. Fifty ml of dibutyl phthalate was added as

solvent and 0.6 g of *p*-toluenesulfonic acid monohydrate as catalyst. The reaction mixture was heated to 130 °C and DOL and water were collected as an azeotrope at 72 °C. The percent composition of the azeotrope is 93 % DOL and 7% water.

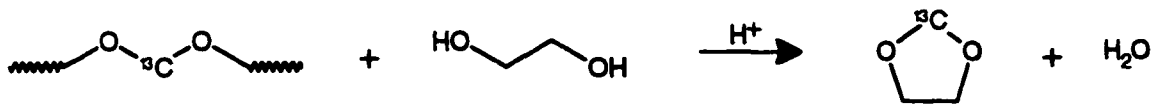

The DOL was dried first with anhydrous $CaCl_2$ to remove most of the water and then by distillation from CaH_2. The final yield was 65%. The purity of the ^{13}C labeled DOL was ascertained based on NMR spectra. Figure III B-2 shows ^{13}C NMR spectra for two coplymerization systems , both with the same comonomer feeds. In the upper spectrum the DOL is not enriched ; in the lower spectrum the DOL is enriched to 33%.

COPOLYMER SYNTHESIS

The reaction tubes, septa, and stir bars were dried under vacuum overnight at 70°C. Hot dry TOX (~6g) (water level less than ~13ppm by weight) was injected into warm tared reaction tubes. The exact mass of tube and trioxane was recorded and the tube was placed in a 65°C oil bath. The desired feed of dry dioxolane was then injected through the septum into the TOX.

For polymerizations followed directly using NMR, one spectrum was acquired prior to the addition of initiator. Immediately afterwards the sample was initiated and acquisition was begun. In the postcloud point studies the samples

were kept in a 65° temperature bath, were initiated and allowed to proceed to the desired conversion as judged by the degree of transparency of the system. The polymerizations were quenched by plunging the reaction tubes into liquid nitrogen where it remained for 30 minutes to 1 hour. Immediately after removing the tubes from the dewar the samples were ground in a SPEX liquid nitrogen freezer mill. At this point some samples were dissolved in a solution of N,N-dimethylformamide (50%), benzyl alcohol (49%) and triethanolamine (1%) at 175°C for 1 hour. This process served the dual purpose of removing the unstable hemiacetal chain ends as well as destroying any remaining initiator. After precipitation, the polymer was washed repeatedly with acetone and methanol (usually twice with acetone and twice with methanol) until the precipitated polymer was white in color. The polymer was then dried by vacuum overnight at 60°C. The remaining samples were analyzed without further treatment.

NMR

^{13}C NMR spectra of the precloud copolymerization were obtained on bulk samples at 70°C using a Varian Unity Plus-300 spectrometer operating at a ^{13}C resonance frequency of 75 MHz. The quenched sample spectra were obtained on either a Bruker WP200 SY spectrometer operating at a ^{13}C resonance frequency of 50.13 MHz or a Varian Unity Plus-500 spectrometer operating at 125.723 MHz.. The copolymer samples were first dissolved in a minimum volume of 1,1,1,3,3,3-hexafluoro-2-propanol (HFIP). When a clear solution was achieved, deuterated

chloroform was added as a lock solvent. The spectra were acquired in a temperature range of 40-45°C. For samples studied directly after quenching, $Cr(AcAc)_3$ (1 wt %) was added as a relaxation agent in some cases to ascertain the influence of variation in relaxation time for ^{13}C nuclei of different species. The chemical shift was referenced on the TOX resonance at 93.234ppm which was itself calibrated on the chloroform triplet at 77.00ppm.

The average sequence length of M units was calculated using the following equation[2].

$$\overline{L_M} = \frac{P\{M\}}{P\{MME\} + P\{EME\}}$$

Where *P{M}*, *P{MME}* and *P{EME}* are the probabilities of forming any M centered triad, the MME triad and the EME triad, respectively. Theoretical curves for the pentad frequency vs. E unit incorporation were prepared using first order Markov statistics with the following constraints:

$$P_{ME} = E_{incorp.}$$

$$P_{EM} = 1$$

The first equation states that the probability that an E unit will follow an M unit is equal to the mole fraction of E units incorporated in the chain. The second equation states that every E unit must be followed by an M unit.

RESULTS AND DISCUSSION

PRECLOUD PERIOD

Under specific conditions of comonomer ratio and initiator concentration, the reaction is sufficiently slow to allow *in situ* quantitation of monomer and polymer species using ^{13}C NMR. Bulk copolymerizations were carried out at 9:1 mole ratio methylene oxide to ethylene oxide using $BF_3O(Bu)_2$, $MoO_2(acac)_2$ and triflic anhydride ($(CF_3SO_2)_2O$) as initiators, and at a 19:1 mole ratio using $BF_3O(Bu)_2$. Additional copolymerizations were carried out using dioxolane which was isotopically enriched to 30% with ^{13}C on the acetal carbon. For these copolymerizations only $BF_3O(Bu)_2$ was used as initiator.

Although NMR has been applied previously to study the bulk copolymerization of TOX with DOL, relatively low field ^{1}H NMR was used and complete resolution of some of the species involved in the process was not possible. However, since those studies were completed, improvements in NMR technology include increased field strengths and stability as well as better line shape and sensitivity. These improvements coupled together can be used to explore this copolymerization further. Most importantly, because the field drifts so little in the unlocked mode (1 Hz/24 hrs.), running relatively long ^{13}C acquisitions is now possible on bulk samples. The resulting spectra show complete resolution of the resonances of all of the methylene species (Table III B-1). Furthermore, the polymer pentad sequences are partially resolved, yielding relative intensities for the heptad sequences. Figure III B-3 represents a typical spectrum acquired during a copolymerization.

Table III B-1. Methylene species resolved by ^{13}C NMR during copolymerization of trioxane and dioxolane.

SPECIES	NAME	CHEMICAL SHIFT (PPM)
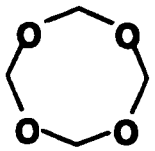	TEX	96.21†
MEMEM		95.35
	DOL	94.50
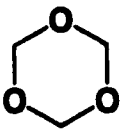	TOX	93.23
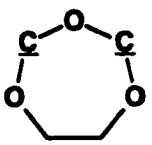	TOP	92.71
MEMMM		92.58
MEMME		92.12
MMMMM		89.69
EMMMM		89.25
EMMME		88.76

† The resonance from tetraoxane is broadened by the rapid conversion which occurs between its boat and chair conformations.[3]

Kinetic curves of each of the above methylene species were constructed from the time series of NMR spectra acquired during copolymerization. Figure III B-4. shows the curves from a polymerization system initiated with $BF_3O(Bu)_2$. The data suggest that the "precloud period" can be further divided into three shorter stages, during which substantially different processes occur. The first stage begins when initiator is injected into the system and is distinct in that during this period no polymerization occurs. Instead, the number of comonomers in the system

increases from two to five. This occurs as the following reactions take place: (1) Initiator attacks trioxane which then decomposes yielding formaldehyde, (2) Formaldehyde is inserted into DOL to yield trioxepane(TOP), (3) Formaldehyde is inserted into TOX to yield Tetraoxane(TEX).

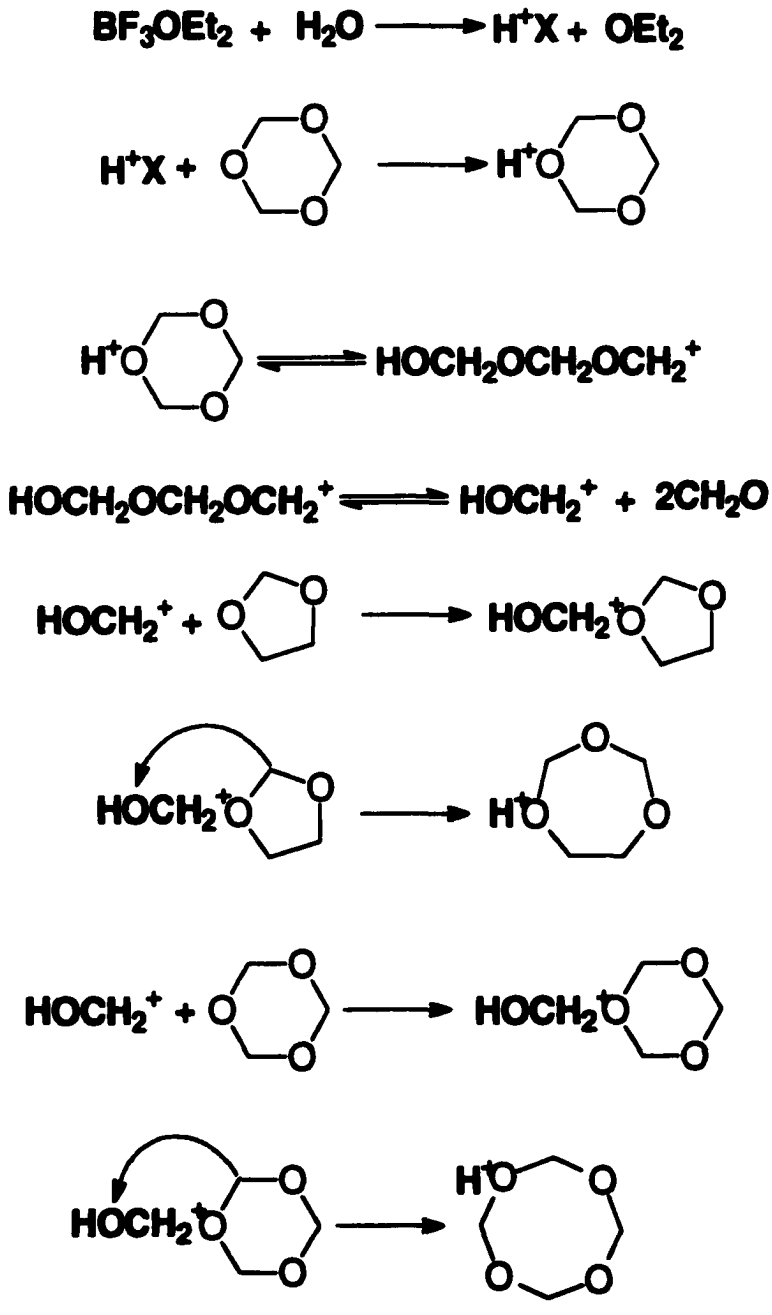

Figure III B-5. Reactions for secondary monomer formation

This stage ends when approximately 25% of the DOL has been converted to TOP. Quantifying the concentrations of formaldehyde and TEX at the end of the stage was not possible. In the case of formaldehyde the concentration is too low to be observed by the methods employed. Although present at significantly higher concentration levels than formaldehyde, TEX resonances could not be accurately integrated due to its broad line width (50 Hz). Nevertheless, it is clear that its concentration never exceeds 1 mole%.

The dynamic nature of this stage is evident in the plot shown in Figure III B-6. Four kinetic curves are displayed for a TOX /DOL polymerization where the DOL was 30% ^{13}C enriched. The black symbols represent the amount of monomer present as determined directly by the methylene oxide resonance. The red symbols represent the calculated amount of monomer present obtained by the intensity of ethylene oxide units multiplied by 15. The factor 15 is to account for the 30 % ^{13}C enrichment at C-1 for DOL which contains ethylene oxide protons and methylene protons at a ratio of 2-to-1. An immediate divergence of the DOL curves occurs because the ^{13}C labeled methylene oxide units are being distributed into the reaction system through fast exchanges of formaldehyde among the species involved in the copolymerization. Initially this is not observed in the TOP because TOP is still approaching its equilibrium concentration. However in the later stages of the reaction, the TOP curves also diverge.

The beginning of the second stage is marked by the onset of polymer formation. All methylene centered pentads appear simultaneously, with the exception of the EMMME pentad, which appears slightly later. This indicates that all five of the monomers participate in the polymerization during this stage. Early on, TOP reaches its maximum concentration and then starts to recede. Also at this stage, DOL is consumed at the fastest rate. This is directly reflected by the rate of increase of pentads containing two E units (MEMEM, EMMEM, EMMME), growing at their greatest rate during this period.

The final stage begins when the rapid decrease in DOL concentration and rapid growth of two-E pentads levels off. For the remainder of the precloud period the concentration of pentads containing two-E units remains nearly constant, or shows slight declines. The concentrations of TOP and DOL both decline at similar slow rates and are present in almost equal amounts.

Figure III B-7 shows the possible sequences that each of the monomers might form as it polymerizes. For DOL and TOP the sequences produced are limited to those shown because every propagating sequence must end with an M unit. TOP unlike the other monomers has two routes by which it can be incorporated .

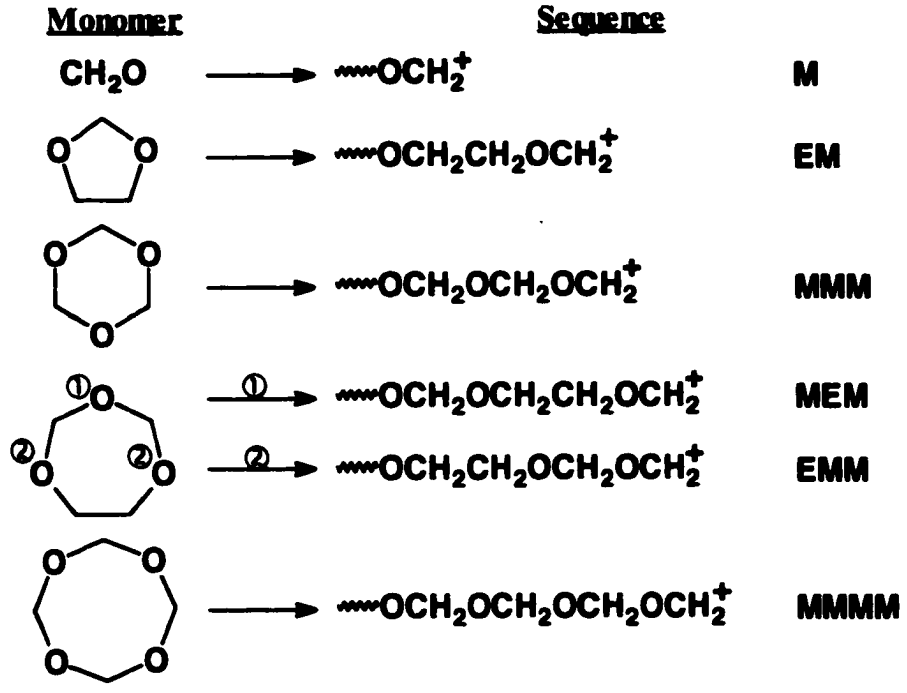

Figure III-B 7. Monomers and their incorporation into the polymer sequences

Attack on site ② of DOL is preferred statistically as well as chemically, because of the higher basicity of this site relative to ①.

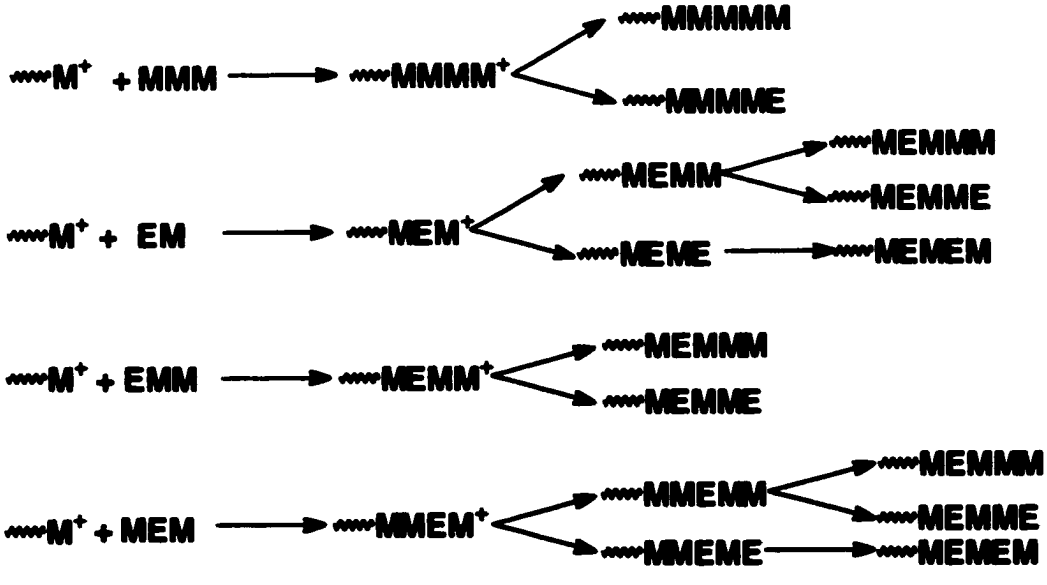

Figure III B-8. Pentad sequences possible from each monomer

Figure III B-8 shows all of the possible pentad sequences that can arise from the addition of each monomer. During the onset of polymerization at the start of the second stage, DOL and TOP are preferentially incorporated into the growing polymer chain. This is a consequence of their higher basicity and relative reactivities compared with TOX. Thus, the polymer produced is relatively rich in E units, resulting in many pentads that contain two E units. When the combined concentration of DOL and TOP drops to approximately 15 mole % based on TOX, the number of pentads containing 2 E units levels off. Throughout the remainder of the "precloud period" the number of two-E pentads remains almost constant while the number one-E pentads and five-M pentads continues to increase. The rate that single-E pentads form during this stage suggests that they result from the formation of new copolymer rather than from rescrambling. This can be understood by considering how the spacing of E units in the copolymer backbone dictates the pentads formed. In the sequence shown below the center E unit is separated from the two nearest E units by 4 M units. This one E unit results in the formation of four M centered pentads (boxed).

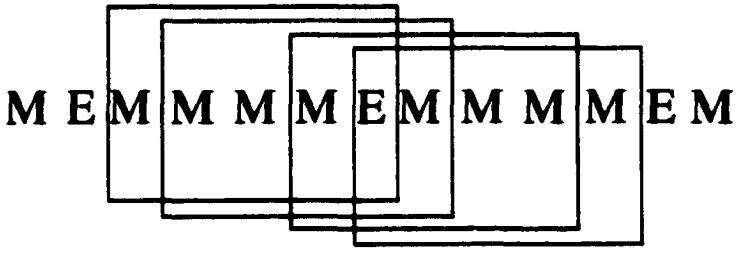

Therefore when E units are incorporated with a minimum separation of four M units, the rate that single-E pentads are formed should be four times the rate at which DOL+TOP are consumed: Table III B-2. shows the rates of change of concentrations for the monomers and polymer sequences during the three stages. The values of Mole% are expressed based on the total number of moles of methylene oxide units in the system.

Table III B-2. Rates of change of concentrations for monomer and polymer sequences (mole%/minute)

SPECIES	First stage 10 -80 min	Second stage 100 -170 min	Third stage 170- 245min
TRIOXANE*	-0.037/-0.012	-0.282/-.094	-0.177/-0.059
DIOXOLANE	-0.035	-0.049	-0.010
TRIOXEPANE*	0.061/0.030	-0.026/-0.009	-0.011/-0.006
MMMMM	not present	0.109	0.093
MEMMM	not present	0.078	0.019
EMMMM	not present	0.064	0.023
EMMEM	not present	0.018	0.0
MEMEM	not present	0.007	-0.003
EMMME	not present	0.007	-0.002

*The top number indicates methylene carbons while the bottom is the entire ring

The Table shows that during the second stage the ratio of consumption of TOX to E-containing monomer (DOL and TOP) is 1.5 to 1. However, during the third stage this ratio increases dramatically to 4.5 to 1. If E units were spaced

evenly they would be separated by 5 M units during the second period and 14 during the third. When the rate that the single-E pentads are formed (10.7×10^{-4} mole% / sec) is compared with the combined rate of DOL and TOP consumption (-2.58×10^{-4} mole%/sec) for the third stage, we see that single E pentads form 4 times faster than DOL and TOP are consumed. As discussed previously this is what is expected if the E units are spaced further than 4 units apart. This, combined with the fact that there is no significant decrease in the number of double-E pentads during this stage suggests that transacetalization is not substantially redistributing the E units that are already part of polymer chains. Instead, one-E pentads form as DOL and TOP continue to be incorporated, but at a lower rate relative to TOX.

POST CLOUD PERIOD

Table 3 summarizes polymerization conditions for ninteen copolymerizations, including the state of the sample when it was quenched and incorporation results. All of the samples were quenched in liquid nitrogen except MWB2P983 and MWB2P984. They were quenched by adding small amounts of their bulk liquids to NMR tubes each containing a solution of chloroform-d, HFIP and a small amount of triethylamine. The resulting solutions were then analyzed directly by ^{1}H and ^{13}C NMR spectroscopy. Twelve of the samples were dissolved in a solution of N,N-dimethylformamide(50%), benzyl alcohol(49%) and

triethanolamine(1%) at 175°C for one hour(hydrolyzed) after quenching. This process removed all monomer, soluble copolymer and unstable hemiacetal chain ends from the insoluble copolymer. What remained was the thermally stable portion of the insoluble copolymer.

Table 3 shows that for every case that was quenched before 100 % conversion was reached, the mole % of DOL incorporated in the copolymer exceeded the mole% of DOL in the original feed. However, for the experiments that were allowed to reach 100% conversion the DOL incorporated was less than what was originally in the feed. The first observation can be readily explained by the preferential incorporation of E units during the early stages of the polymerization, so that at any point during the copolymerization the polymer contains a relatively high mole fraction of E units in relation to the initial feed. As the polymerization proceeds the mole fraction of E units in the copolymer continues to decrease as more TOX is incorporated. Ideally, when 100% conversion is reached the incorporation ratio should equal the feed ratio, since no monomer leaves the system during polymerization. This is, however, not observed, perhaps due to loss of E-rich species in the hydrolysis process. During the hydrolysis process the sample is dissolved and reprecipitated and then washed several times with acetone and methanol. It is likely that some E-rich soluble copolymer or oligomer, formed early in the polymerization, remains at the end and is washed out.

Table 2 Polymerization and NMR conditions

#	SAMPLE	DOL Feed[1]	Initiator	Initiator to TOX	State	Conv.	NMR	DOL inc.	avg M seq det by M	avg. M sep det by E	$\frac{\text{Avg M seq}_M}{\text{Avg M seq}_E}$
1	MWB2P103-20	8	BF_3OBu_2	100ppm	S	70[2]	Unhydrol	0.107	8.27	8.35	0.99
2	MWB2P103-19	8	BF_3OBu_2	100ppm	G	64[2]	Unhydrol	0.111	7.76	8.01	0.97
3	MWB2P103-16	8	BF_3OBu_2	100ppm	G	63[2]	Unhydrol	0.111	8.51	8.01	1.06
4	MWB2P103-18	10	BF_3OBu_2	100ppm	S	100*	Hydrol	0.098	8.76	9.20	0.95
5	MWB2P102-13	10	MoO_2	100ppm	S	100*	Hydrol	0.089	9.96	10.23	0.97
6	MWB2P102-6	10	Triflic acid	17.2ppm	S	100*	Hydrol	0.082	10.55	11.19	0.94
7	MWB2P984	5	BF_3OBu_2	100ppm	C	30[2]	Unhydrol	0.132	5.41	6.58	0.82
8	MWB2P983	5	BF_3OBu_2	100ppm	C	25[2]	Unhydrol	0.14	4.73	6.14	0.77
9	MWB2P962	5	BF_3OBu_2	100ppm	S	46†	Unhydrol	0.088	9.81	10.36	0.94
10	MWB2P961	5	BF_3OBu_2	100ppm	G	69†	Unhydrol	0.112	8.15	7.93	1.03
11	MWB2P882	5	BF_3OET_2	100ppm	G	28‡	Hydrol	0.109	8.10	8.17	0.99
12	MWB2P881	5	BF_3OET_2	100ppm	G	49‡	Hydrol	0.096	8.69	9.42	0.92
13	MWB2P84C1	5	BF_3OBu_2	65ppm	G	61[2]	Hydrol	0.07	11.34	13.29	0.85
14	MWB2P84C2	5	BF_3OBu_2	65ppm	G	61[2]	Hydrol	0.069	12.58	13.49	0.93
15	MWB2P821	5	BF_3OBu_2	110ppm	G	47[2]	Hydrol	0.097	9.71	9.31	1.04
16	MWB2P82C	5	BF_3OBu_2	110ppm	G	47[2]	Hydrol	0.084	9.90	10.90	0.91
17	MWB2P80	5	BF_3OBu_2	1150ppm	S	~	Hydrol	0.077	13.00	11.99	1.08
18	MWB2P783	5	BF_3OBu_2	867ppm	S	100*	Hydrol	0.045	22.21	21.22	1.05
19	MWB2P781	5	BF_3OBu_2	800ppm	S	100*	Hydrol	0.046	21.93	21.74	1.06

[1] Feed and incorporation are mol based on Formaldehyde [2] Determined by NMR, conversion of TOX only.

† Remained after being placed under vacuum for 20 hours at 65°C ‡ Remained after hydrolysis

* Experiment not quenched or quenched after completion(#18), C=clear, G=light white gel, S=appeared solid

This scenario is further supported through a comparison of copolymer pentad incorporations with first order Markov distribution curves (Figure III B-8). If a perfect fit is achieved the E units are distributed randomly with the only constraint that every E unit must be followed by an M unit. In Figure III B-8, the experiments are broken down into two groups, hydrolyzed (Δ, O) and nonhydrolyzed (□,◊). With the exception of the samples quenched while still clear, both sets of data generally fit the curves well. Nevertheless, for almost all samples the number of double-E pentads is higher than predicted. This observation, coupled with data from the precloud point period, argues that the randomization process is not complete, although more effective during the post cloud point period. Accordingly, the survival of some of the E- rich chains does seem probable.

CONCLUSIONS

It is clear that transacetalization does not significantly contribute to randomization during the "precloud period" and that the sequence distribution of copolymer samples quenched during the postcloud period are close to random. Therefore transacetalization must occur in or on the crystal surface as polymerization and crystallization occur simultaneously. If the E-units are restricted for the most part to the surface of the crystal and TOX is inserted into them at the crystal surface the E-units will be moved further from one another. However, when two E units are in close proximity, as in a two-E pentad, they may

survive as such since the whole unit may be lifted as the crystal grows in thickness. Such a process is favored thermodynamically since it would yield larger and more perfect crystals. In addition some E-rich polymer (soluble) formed early in the polymerization may not participate in this process since it is not crystalline.

References

[1] Jaacks, V. *Adv. Chem. Ser.*, 1969, **91**, 371

[2] Yamashita, Y., Asakura, T., Okada, M., Ito, K. *Makromol. Chemie*, 1969, **129**, 1

[3] Dale, J., Ekeland, T., Krane, J. *J. Am. Chem. Soc.*, 1972, **94**, 1389

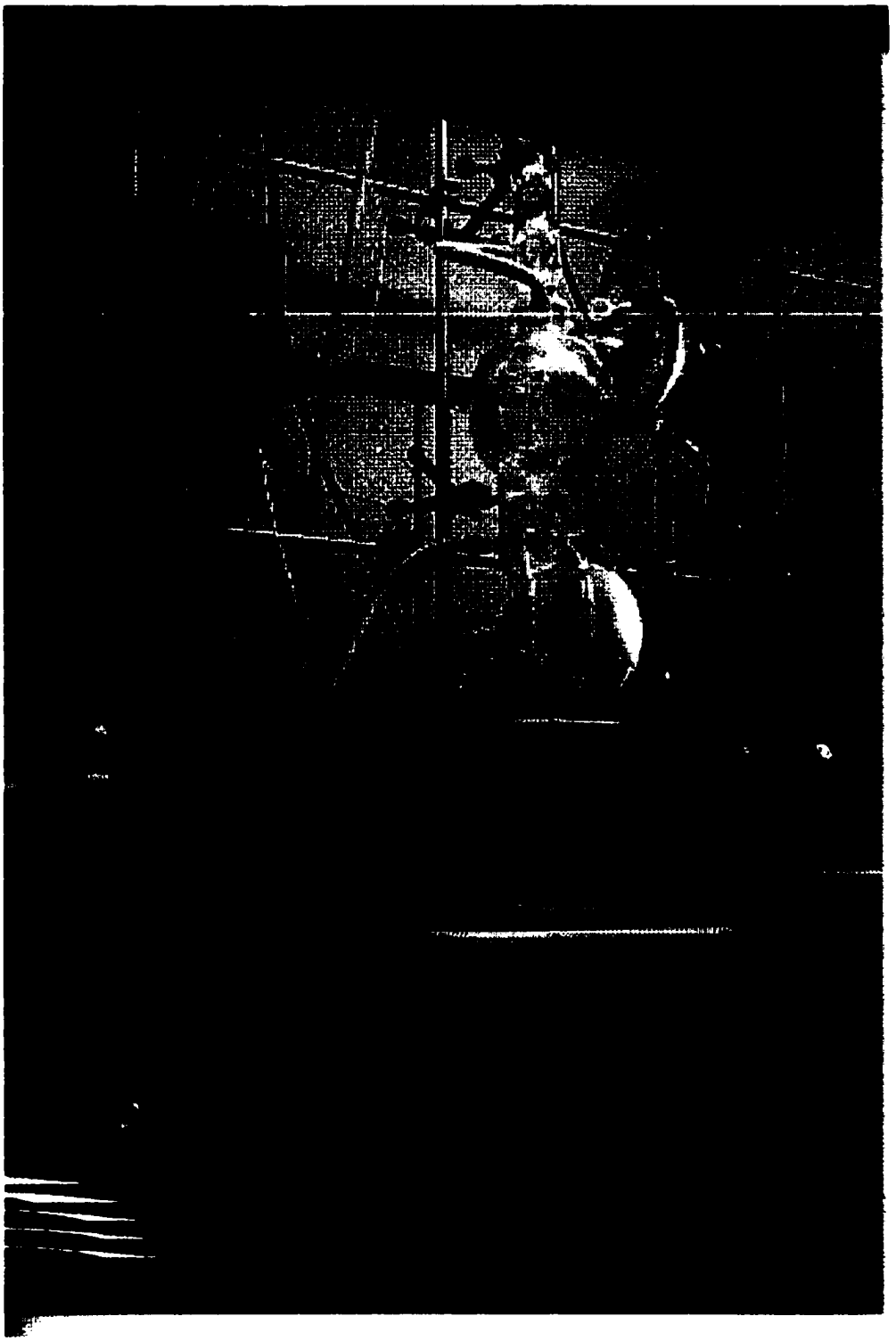

Figure III B-1. Still head designed to continuously reflux trioxane over NaK amalgam. 80 °C silicon oil circulated through the outer jacket to keep the trioxane from crystallizing. The inside of the apparatus was maintained under a positive pressure of dry argon.

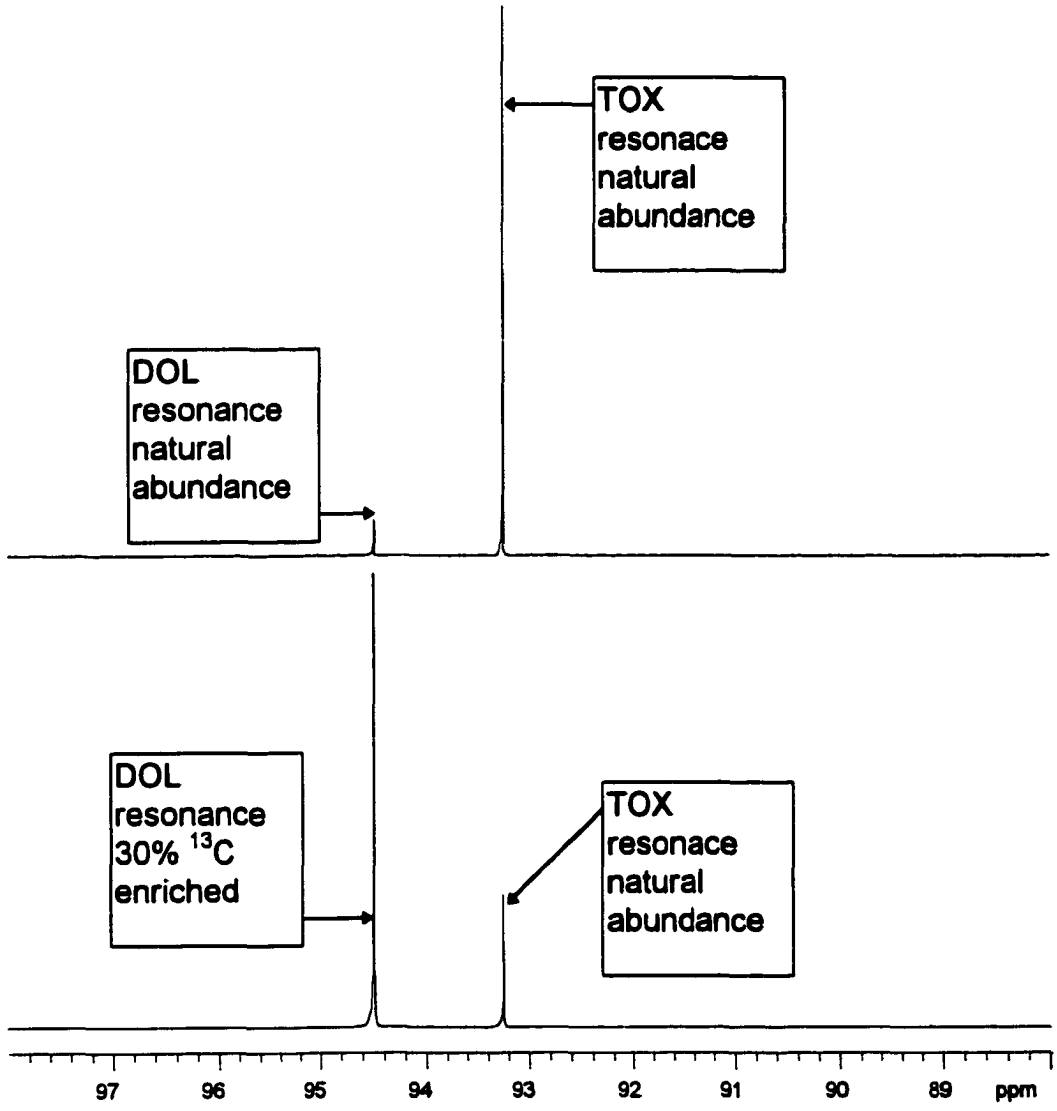

Figure III B-2. ^{13}C spectra of TOX-DOL copolymerization (M region). M to E feed ratio 10:1 in both spectra. In the lower spectrum 30% of the DOL methylene oxides have been ^{13}C enriched.

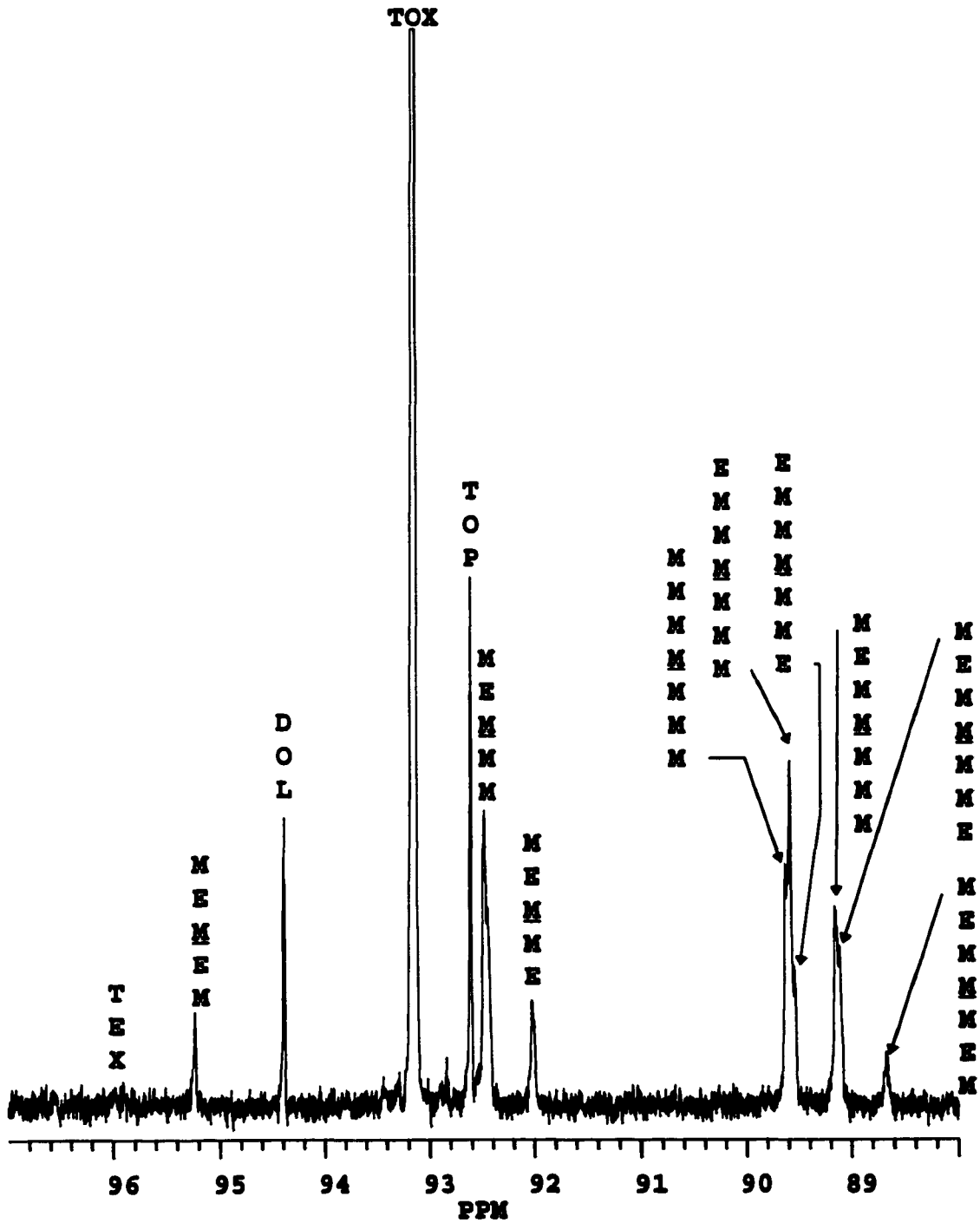

Figure III-B-3. 75-MHz ^{13}C NMR spectrum of the oxymethylene carbons during the bulk copolymerization of TOX-DOL (mole ratio=3:1) at 70 °C. $[BF_3OBu_2]$ = 20 ppm. Acquired 112 min after inititation.

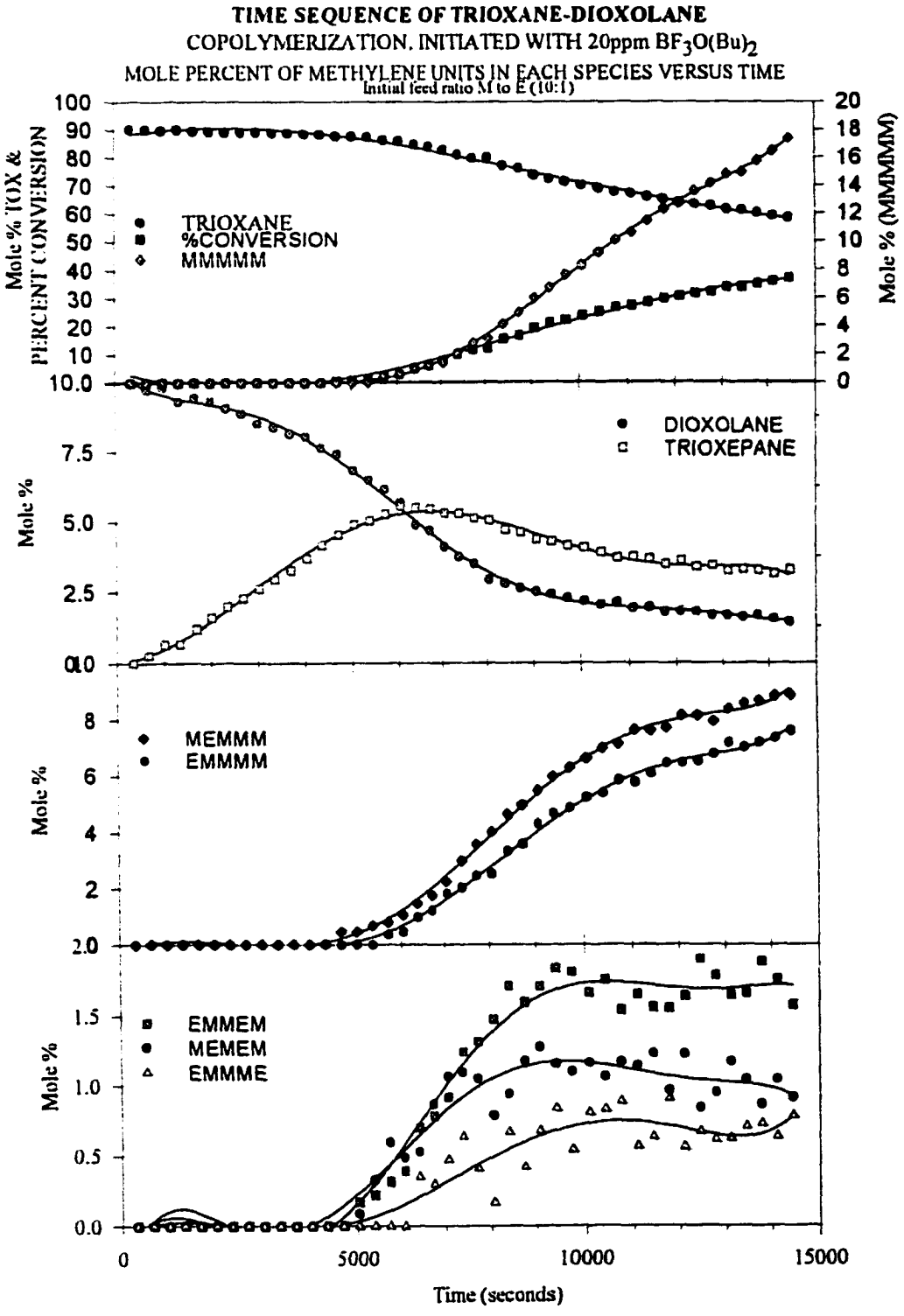

Figure III-B-4. Kinetic curves of Trioxane-Dioxolane copolymerization, initiated with 20 ppm BF_3OBu_2 mole percent of methylene units in each species versus time. Initial feed ratio of M to E (10:1)

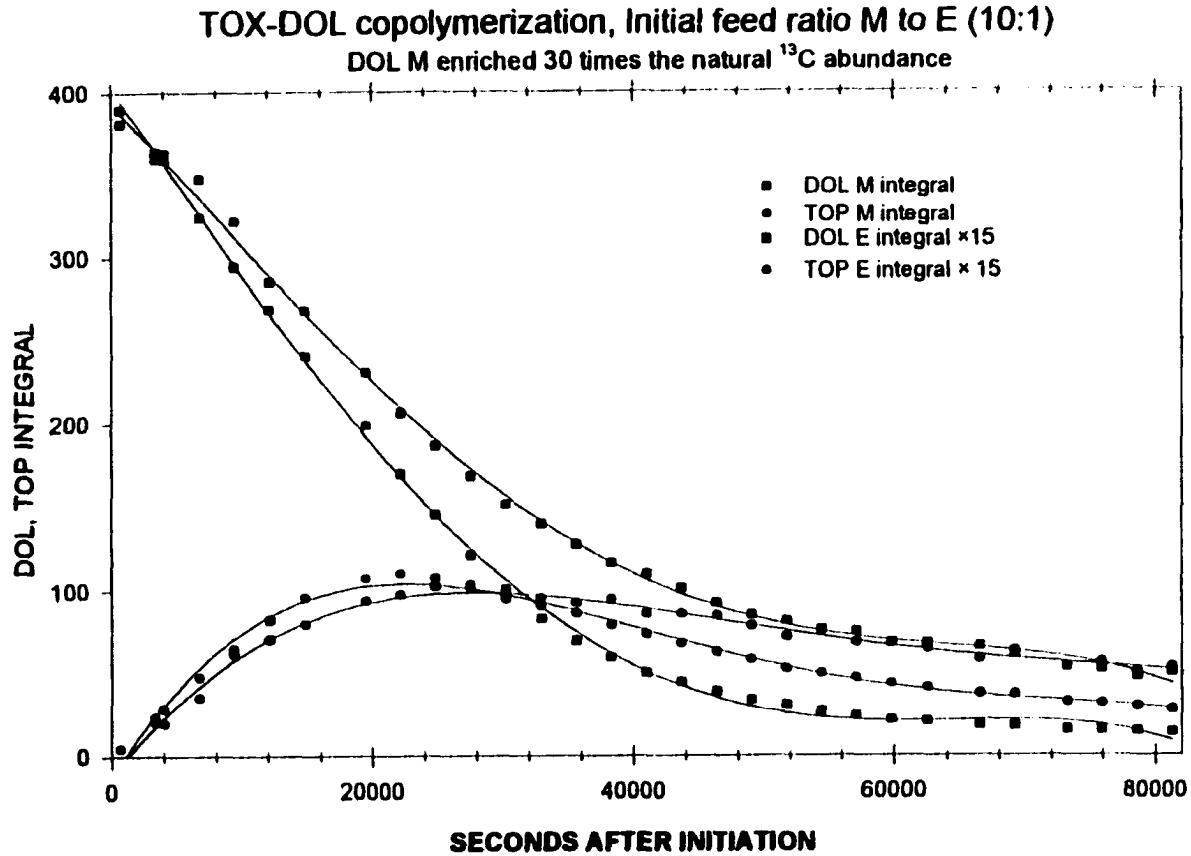

Figure III-B-6. Black curves represent the relative numbers of ^{13}C atoms present in DOL and TOP over the course of the polymerization. The red curves were calculated by multiplying the Ethylene oxide integral for each species by 15. The divergence between the red and black curves indicates a loss of ^{13}C labeled methylene oxide from the monomer.

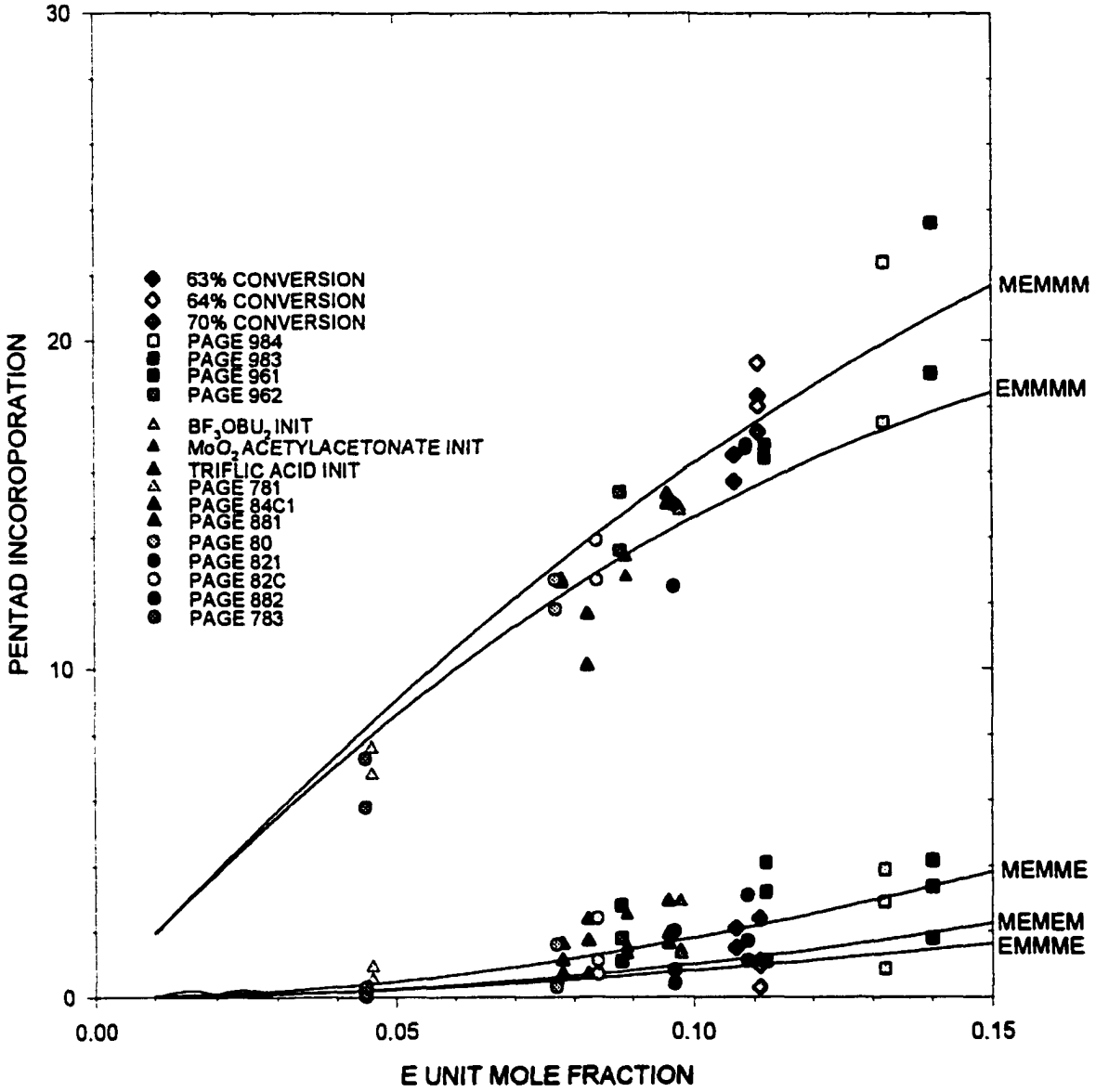

Figure III-B-8. Pentad incorporation data from copolymer samples compared to modified first order Markov distribution curves. Samples represented by Δ's and O 's were hydrolyzed before NMR spectra were acquired, samples represented by ◊ 's and □ 's were not.

C) COPOLYMERIZATION OF TRIOXANE AND 1,5,7,11-TETRAOXASPIRO[5,5]UNDECANE

INTRODUCTION

For a number of years spiro orthocarbonates have attracted considerable interest as monomers which expand or undergo zero shrinkage during polymerization[1]. Most of the past work has focused on the homopolymerization and block copolymerization of these monomers. This report describes the first cationic copolymerization of 1,5,7,11-tetraoxaspiro[5,5]undecane (SOC) with trioxane (TOX).

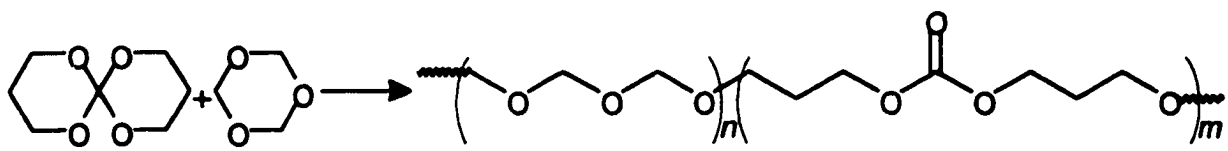

SOC TOX COPOLYMER

EXPERIMENTAL

GENERAL

All chemicals were purchased from Aldrich Chemical Company at the highest purity available and used as supplied unless indicated otherwise. All operations were carried out under dry nitrogen inside a glove box when air sensitive compounds were involved. Such compounds included 1,5,7,11-tetraoxaspiro[5,5]undecane, an unsubstituted six-membered spiro orthocarbonate.

SYNTHESIS OF 1,5,7,11-TETRAOXASPIRO[5,5]UNDECANE

Triethylamine and 1,3-propanediol were dried over calcium hydride and distilled under nitrogen. The catalyst used, p-toluenesulfonic acid monohydrate, was heated to 100 °C for four hours under vacuum to prepare the anhydride[2]. The SOC monomer was synthesized using acid catalyzed transesterification of tetramethyl orthocarbonate with 1,3-propanediol[3]:

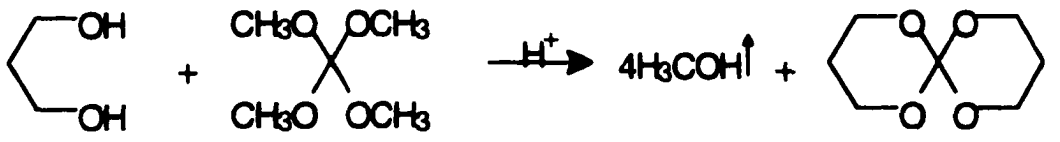

1,3-PROPANEDIOL TETRAMETHYL ORTHOCARBONATE SOC

A solution of tetramethyl orthocarbonate (24.9g, 183 mmol), 1,3-propanediol (27.9 g, 366 mmol), p-toluenesulfonic acid anhydride (0.3g), and dibutyl phthalate (60 ml) was allowed to react at 110 °C under stirring in a distillation apparatus until no additional methanol was collected (approximately 4 hours). Then, 0.6 ml of triethylamine was added to the solution after cooling to room temperature. The reaction system was left standing at room temperature overnight without stirring under a continuous flow of nitrogen. The resulting product, SOC, crystallized from the reaction mixture by the next morning. The crude crystals were collected by filtration, and then dissolved in acetone. Approximately an equal volume of hexane was added to the solution and acetone

was then evaporated by heating until crystals appeared. The SOC recrystallized as colorless needle-like crystals upon cooling. The crystals were washed with cold hexane and dried overnight *in vacuo*.

SYNTHESIS OF COPOLYMER AND SOC HOMOPOLYMER

TOX was dried over sodium and distilled under dry nitrogen. The solvent used for copolymerization ,1,2-dichloroethane, was dried over calcium hydride and distilled under dry nitrogen. The required amounts of TOX, SOC and dichloroethane were placed into a 25X150 mm test tube. The tube was sealed with a septum and swirled until the contents dissolved (10-30min). In some experiments the resulting solution was used directly while in others it was aliquoted into equal portions for duplicate experiments. Each tube was provided with a magnetic stirrer. The tubes were placed in a 60 °C oil bath and stirred for 15 minutes before the addition of initiator. Two different initiators were used. Twenty μL of boron trifluoride etherate was injected through the septa into the reaction solution. Additional 20 μL injections were administered at 15 minute intervals until the solution began to cloud (usually 60-100 μL were used). Once clouding occurred no further additions were made. For the second initiator, 0.71 M triflic anhydride in dry toluene was injected (17 μl) . After initiation all tubes were left overnight for copolymerization at 60°C. The resulting polymers were removed from the reaction tubes, crushed with a spatula and placed in 20 ml of methanol containing 1% triethanolamine (TEA). The mixtures were stirred at

room temperature for 30 minutes to destroy any remaining initiator. Then the methanol was filtered off. For copolymerizations with SOC feeds greater than 3 mole %, two fractions of copolymer resulted. One, SOC rich which was soluble in acetone, and the other, acetal rich and insoluble in all common organic solvents except at high temperature. In most of the copolymerizations only the insoluble product was isolated. It was collected by filtration, washed the twice with acetone and twice with methanol and then dried at 60-70 °C *in vacuo* for one to four hours.

SOC was homopolymerized in a manner similar to that used for the copolymerization. In a dry box, SOC (2.13 g), dry methylene chloride (5 ml) and a stir bar were placed in a reaction tube. The tube was sealed with a septum and placed in a 40 °C oil bath. Twenty μl of $BF_3(OEt_2)$ was injected after all of the monomer had dissolved, and the solution was stirred for 2 days at 40 °C. One ml of triethylamine was then added to the solution to quench the reaction. After evaporating the CH_2Cl_2 and TEA the homopolymer was collected as a colorless viscous material. This material was redissolved in a minimum volume of CH_2Cl_2 and added dropwise to methanol to precipitate the polymer. An oily precipitate was collected and dried overnight at 70°C *in vacuo*.

HYDROLYSIS OF ACETAL RICH FRACTION OF COPOLYMER

Unstable hemiacetal chain ends were removed from the copolymer using a procedure described as follows. The copolymer (3-6 g), dimethyl formamide

(12.5ml) and benzyl alcohol containing 2% by volume triethanolamine (12.5ml) were placed in a 50 ml round bottom flask equipped with an air cooled condenser. The mixture was heated to 175±5°C under magnetic stirring to dissolve the copolymer (~15 min.), and allowed to react at this temperature for one hour. The flask was removed from the oil bath and cooled to room temperature under stirring. The copolymer was collected by filtration and washed with acetone and methanol to remove the solvents. The resulting product was dried at 60-70°C *in vacuo* overnight.

CHARACTERIZATION

NMR spectra of the SOC monomer and the acetal rich fraction of copolymer were acquired on an IBM WP-200 NMR spectrometer operating at a proton resonance frequency of 200 MHz. The SOC monomer ^{1}H spectrum was acquired at room temperature with chloroform-d as solvent. The ^{1}H spectra of the acetal rich copolymers were acquired at 120°C with DMSO-d_6 as solvent; and the ^{13}C spectra were acquired at room temperature with hexafluoroisopropanol as solvent. ^{1}H and ^{13}C NMR experiments were performed on the SOC-rich fraction of copolymer at 500 and 125 MHz, respectively, on a Varian Unity Plus-500 spectrometer. The sample was dissolved at 30°C in chloroform-d. The experiments performed include: two-dimensional homonuclear J-resolved to show the ^{1}H coupling pattern, heteronuclear multiple quantum coherence (HMQC)[4,5] to determine the ^{1}H-^{13}C single bond correlations, and heteronuclear multiple bond

coherence (HMBC)[6,7] to make long range ^{1}H-^{13}C correlations. The HMBC experiment was optimized to show correlations on the order of 9 Hz. The course of copolymerization was observed *in situ* by ^{1}H NMR on the Varian Unity Plus-500. A solution of the monomers (3.97M TOX, 0.198M SOC) was prepared in chloroform-d, then initiated with $BF_3O(Bu)_2$ ($2.7x10^{-2}$mol %). Eighty-five spectra were acquired at 160sec intervals starting immediately after initiation.

The molecular weights of the insoluble copolymers were estimated using the Mark-Houwink equation and a relationship between [η] and the η_{inh} for ethylene oxide-trioxane copolymers in HFIP (0.200 g/dl) at 25°C. The nominal molecular weight of the SOC-rich fraction of copolymer was estimated by gel permeation chromatography performed on a Waters Model 150C/GPC using tetrahydrofuran as solvent.

Themogravimetric analysis was performed on a Thermal Analysis Instruments Hi-Res TGA model 2950. Samples weighing from 4 to 6 mg were purged inside the cell for 10 min with nitrogen prior to heating at 10°C/min. A N_2 flow of 100 ml/min. was maintained throughout each run.

The heat of fusion and apparent percent crystallinity were determined with a Dupont Instruments DSC model 2910 equipped with a LNCA II liquid nitrogen cooling assembly. Samples weighing approximately 5 mg were heated at 10° C/min to 190°C to obtain thermograms which reflect the properties of solution-crystallized polymer. Each sample was then cooled at 4°C/min to 40°C and

reheated at 10°C/min to 190°C to acquire thermograms of melt-crystallized polymer. The same cycle was repeated a third time to verify the reproducibility of the melt-crystallized thermogram. A weighed Indium sample(10.27mg) was run as the standard and the percent crystallinity was based on a heat of fusion ΔH_f of $2.46x10^2$J/g for 100% crystalline polyoxymethylene[8].

Infrared spectra of copolymer KBr Pellets were collected on a BIO-RAD FTS-40 Fourier transform infrared spectrometer.

3.RESULTS AND DISCUSSION

VERIFICATION OF SOC STRUCTURE

The reaction yielded 16.3g (55%) of colorless needle-like crystals with a melting point of 128 °C (literature value[9] of 132-133°C). Although the melting point of the crystals was lower than that previously reported, the ^{1}H NMR spectrum (Figure III-C-1) of the material verified its purity (δ 1.8, p, 4 H; 4.1, t, 8 H).

STRUCTURE ASSIGNMENT OF THE "INSOLUBLE" ACETAL RICH FRACTION OF TOX-SOC COPOLYMER

The propagating species in SOC homopolymerization is reported to be trioxocarbonium ion[10] via a 1,10-transfer reaction. Shown below is a proposed mechanism for the incorporation of a single SOC monomer into a growing polyacetal chain (Figure III-C-2). Initially, the propagating chain end attacks an SOC oxygen(**O-1**) forming an oxonium ion centered on the SOC oxygen (II). When the bond between the oxygen(**O-1**) and the spiro carbon(**C-6**) opens the

cation is transferred to the spiro carbon(**C-6**), resulting in a trioxocarbonium ion (**III**). Nucleophilic attack of the ion by a TOX molecule then occurs at a methylene carbon(**C-10**) adjacent to one of SOC oxygens in the remaining ring (**IV**). As the ring opens a carbonate unit is produced along with an oxonium ion (**V**). Thus, the incorporation of a SOC comonomer leads to both an ether and a carbonate linkage in the backbone of the main chain (**VI**). For simplicity the active species is shown as an alkoxycarbenium. However, it has been shown that the large majority of active species are in the form of oxonium ions[11].

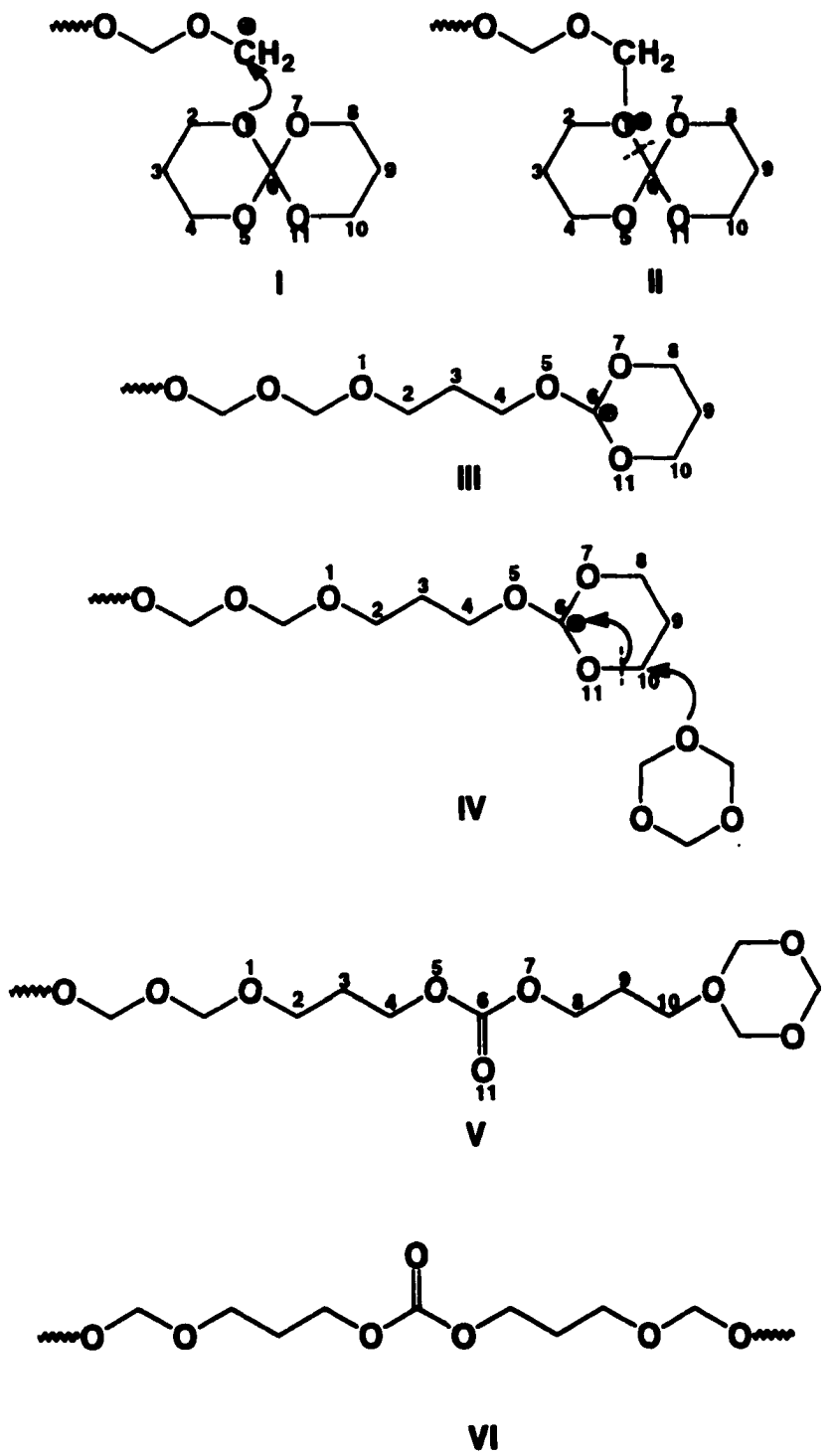

Figure III-C-2. Copolymerization mechanism of TOX and SOC.

The infrared spectrum of the copolymer (Figure III-C-3), shows carbonyl stretching at 1747 cm^{-1} and ether stretching at 1265 cm^{-1}. The carbonyl stretching frequency correlates well with that of diethyl carbonate which absorbs at 1746.9 cm^{-1}. The carbonate carbon is further established by comparing the ^{13}C NMR spectrum with the ^{13}C DEPT-135 NMR spectrum (Figure III-C-4). In the ^{13}C NMR spectrum there is a resonance at 159.6 ppm which does not appear in the DEPT-135 NMR spectrum. Its chemical shift is in the expected region for an alkyl carbonate and the fact that it does not appear in the DEPT spectrum confirms that it has no attached protons. The proton NMR spectrum of the TOX-SOC copolymer (Figure III-C-5) clearly shows the connectivity of SOC with acetal and SOC with SOC. The resonance at 3.61ppm, absent from spectra of both homopolymers, is assigned to H-3′ protons bound to the carbon connecting an SOC comonomer unit with an acetal unit. The assignment is verified through a model polymer consisting only of the repeat units ~(CH_2O)~ and ~($CH_2CH_2CH_2O$)~. The copolymer was prepared by copolymerizing TOX with 5 mole % 1,3-dioxane. A well resolved triplet at 3.61ppm (Figure III-C-6) from the model polymer lends strong support for our assignment of H-3′ being at the junction of a propane unit with an acetal unit. The resonance at 3.47ppm (Figure III-C-5) is assigned to H-3 based on the SOC homopolymer spectrum. The resonances in the region between 1.7 and 2.1ppm are considered to be 2 multiplets due to H-2 and H-2′. Lastly, the broad triplet structure at 4.15 ppm is assigned to

the H-1 and H-1´. As expected the chemical shift difference is largest between the resonances arising from peaks 3 and 3' which are directly bound to functionally different oxygens. Resonances for 2 and 2' partially overlap and resonances for 1 and 1' are difficult to distinguish from each other.

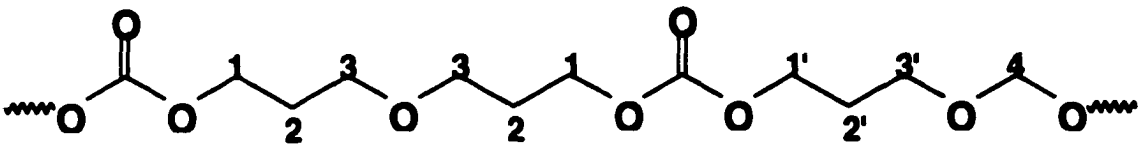

Figure III-C-7 Copolymer structure assignment

COPOLYMERIZATION

The incorporation of SOC into the copolymer was calculated using the following equation.

$$\text{Mole \% incorporation of SOC} = \frac{(\text{Area of peaks 1 \&1'}) / 2}{\text{Area of peak 4} + (\text{Area of peaks 1 \& 1'}) / 2}$$

Table 1 summarizes the feed, initiation conditions , incorporation and yield information, for the copolymerization.

Sample	TOX g	SOC g (mol x10^3)	Initiator	Initiator volume	Initiator conc.	Initial yield*	Hydrolysis loss*	Total yield*	SOC feed†	SOC incorp†
MWB1P50	9.0g (0.30mol)	1.0g (6.24)	$BF_3O(Et)_2$	80µL	2100 ppm	88.7%	42.6%	50.9%	2.0%	1.97%
MWB1P54	8.0g (0.27mol)	2.3g (14.4)	$BF_3O(Et)_2$	160µL	4600 ppm	69.7%	28.2%	50.0%	5.0%	1.84%
MWB1P56A	6.10g (0.203mol)	1.72g (10.7)	$BF_3O(Et)_2$	200µL	3800 ppm	72.3%	30.6%	50.2%	5.0%	1.93%
MWB1P56B	6.10g (0.203mol)	1.72g (10.7)	$BF_3O(Et)_2$	200µL	3800 ppm	76.5%	29.5%	53.9%	5.0%	1.84%
MWB1P62A	4.53g (0.151mol)	2.69g (16.8)	$BF_3O(Et)_2$	200µL	4900 ppm	51.7%	24.9%	38.8%	10.0%	2.2%
MWB1P62B	4.53g (0.151mol)	2.69g (16.8)	$BF_3O(Et)_2$	200µL	4900 ppm	54.8%	30.1%	38.3%	10.0%	2.4%
MWB1P65A	6.35g (0.212mol)	0.343g (2.14)	$BF_3O(Et)_2$	80µL	1500 ppm	84.1%	41.0%	49.6%	1.0%	1.15%
MWB1P65B	6.35g (0.212mol)	0.343g (2.14)	$BF_3O(Et)_2$	80µL	1500 ppm	88.3%	43.2%	50.1%	1.0%	1.01%
MWB1P68A	4.63g (0.154mol)	0.505g (3.15)	$BF_3O(Et)_2$	120µL	3100 ppm	79.6%	38.9%	48.8%	2.0%	1.92%
MWB1P68B	4.63g (0.154mol)	0.505g (3.15)	$BF_3O(Et)_2$	120µL	3100 ppm	79.8%	32.4%	53.9%	2.0%	1.85%
MWB2P26	5.00g (0.167mol)	0.470g (2.93)	Triflic anhydride	2µL	88 ppm	92.3%	39.0%	56.3%	1.7%	1.66%
MWB2P28A	5.37g (0.179mol)	0.19g (1.2)	Triflic anhydride	2µL	66 ppm	94.8%	61.1%	36.9%	0.67%	0.66%
MWB2P28B	4.65g (0.155mol)	0.92g (5.7)	Triflic anhydride	2µL	75 ppm	79.9%	27.6%	57.8%	3.6%	2.48%

*initial yield, hydrolysis loss and total yield are calculated for insoluble copolymer. † SOC feed and incorporation in mole %.

Table 1.Copolymerization of trioxane with 1,5,7,11- tetraoxaspiro[5,5]undecane

SAMPLE	TOTAL YIELD %	HYDR LOSS %	SOC WEIGHT % FEED %	SOC WEIGHT % INC., %	WEIGHT LOSS TGA 1%	WEIGHT LOSS TGA 5%	% CRYSTALLINE (DSC)[1] SOL., MELT	% CRYSTALLINE (DSC)[1] MELT CRYST.	M.P. MELT CRYST.	MOL. WEIGHT
MWB2P28A	**36.9**	**61.1**	**3.4**	**3.4**	**278**	**311**	**85.9**	**81.0**	**168**	**9400**
MWB1P65A	**49.6**	**41.0**	**5.1**	**5.8**	**275**	**304**	**87.9**	**79.4**	**168**	**16800**
MWB1P65B	**50.1**	**43.2**	**5.1**	**5.2**	**246**	**298**	**87.5**	**78.9**	**168**	**16400**
MWB2P26	**56.3**	**39.0**	**8.6**	**8.3**	**289**	**309**	**82.3**	**78.0**	**165**	
MWB1P68A	**48.8**	**38.9**	**9.8**	**9.5**	**280**	**308**	**83.4**	**74.1**	**166**	**14800**
MWB1P68B	**53.9**	**32.4**	**9.8**	**9.1**	**276**	**305**	**82.7**	**71.6**	**166**	
MWB2P28B	**57.8**	**27.6**	**16.5**	**12.0**	**288**	**313**	**81.4**	**77.8**	**160**	**15800**
MWB1P56A	**50.2**	**30.6**	**22.0**	**9.5**	**272**	**305**	**83.9**	**77**	**165**	**7400**
MWB1P56B	**53.9**	**29.5**	**22.0**	**9.1**	**258**	**299**	**86.0**	**79.6**	**165**	
MWB1P54	**50.0**	**28.2**	**22.3**	**9.1**	**276**	**304**	**87.6**	**79.4**	**164**	
MWB1P62A	**38.3**	**24.9**	**37.3**	**10.7**	**291**	**314**	**83.4**	**74.4**	**164**	**6800**
MWB1P62B	**38.3**	**30.1**	**37.3**	**11.6**	**292**	**317**	**84.4**	**77.6**	**163**	
MWB2P31[‡]	**46.9**	**52.2**	**1.2**	**1.2**	**275.6**	**305.6**				

[1]Crystallinities are corrected for weight % SOC, Shaded samples initiated with triflic anhydride [‡]Sample of TOX DOL copolymer

Table 2. Summary of thermal analysis and molecular wt. data

A plot of SOC feed *versus* incorporation in the acetal-rich TOX-SOC copolymer is shown in Figure III-C-8. When the SOC feed is in the range below 2 mole %, incorporation increases with the feed. However, for above 2 mole %, incorporation levels off. When the feed is raised to 5 mole % the incorporation remains at ~2 mole %. Even for a 10 mole % feed, the incorporation does not increase significantly. Table 2 lists samples in order of increasing SOC feed. The significance of the SOC incorporation limit is apparent when the weight % of SOC in the feed is compared to that in the acetal-rich copolymer. A small loss between the feed and incorporation in terms of mole % amounts to a large loss in weight % due to the five-fold difference in monomer molecular weights. Because the incorporation of SOC is limited to ~10 w%, high SOC feeds are found to reduce the total yield of acetal-rich copolymer formed during the polymerization. The effect is most apparent for samples MWB1P62 A and B which had 10 mole % SOC feeds, the highest in the study. However, even though their initial yields are considerably lower than other samples their hydrolysis losses were among the lowest.

The cause of the SOC incorporation limit in the post-hydrolysis copolymer is found in the time series ^{1}H NMR spectra shown in Figure III-C-9. The spectra (acquired during the copolymerization of TOX containing 5 mole % SOC) only show the SOC monomer and polymer methylene peaks. The TOX monomer peak is relatively unchanged during this time and is therefore not included. Spectrum 1

(bottom) shows the monomer solution prior to initiation. Spectrum 2 is of the same solution immediately after initiation with 3000 ppm of $BF_3O(Bu)_2$. Spectra 3, 4, 5 and 6 were acquired at 53, 106, 159 and 212 minutes after initiation, respectively. Examination of the spectra show that even at low SOC feeds the SOC polymerizes almost exclusively at first. This occurs first because the SOC monomer structure with its four oxygens crowded together on the spiro carbon seems to capture almost all of the cationic initiating species. Second, due to its relative instability SOC is much easier to open then TOX and propagation is also dominated by SOC. By comparing the relative sizes of the peaks at 3.34 ppm (SOC homopolymer linkages) and 3.46 ppm (TOX-SOC copolymer linkages), it is clear that even when SOC is present in low concentrations, it is preferentially incorporated to polymer sequences by the growing polymer chain.

Unlike many other monomers which have been copolymerized with TOX, SOC does not possess an acetal unit. Therefore, once sequential SOC units are formed they cannot be redistributed *via* transacetalization and survive as such throughout the polymerization. When the SOC feed is at or below about 2.5 mole % long sequences of SOC units do not occur and the initially formed soluble polymer incorporates more CH_2O units. Because the resulting chain has many acetal linkages dispersed among short SOC blocks and single units, transacetalization redistributes the short blocks and single units throughout the final TOX SOC copolymer (no soluble copolymer). However, when the feed

exceeds 2.5 mole % long blocks of sequential SOC units form, and the resulting chains contain relatively few CH_2O units. These chains remain intact throughout the copolymerization. Therefore the product of the copolymerization is comprised of two fractions: a highly crystalline copolymer consisting primarily of CH_2O units, and an amorphous copolymer with mainly SOC units. When the copolymerization products are worked up by the procedure used to isolate the crystalline portion, and remove its unstable hemiacetal chain ends, the soluble copolymer is simply removed.

Table 3. Structure assignment of the "soluble" soc rich fraction of copolymer nmr oxymethylene sequence assignments

Peak	^{13}C Chemical shift	^{1}H Chemical shift	Triad sequence	Tentative Pentad sequences	Expected long range correlations
4a	89.04	4.860	MMM	MMMMM	4a,4b
4b	88.65	4.843	MMM	SMMMM	4a,4b,4d
4c	88.35	4.826	MMM	SMMMS	4d
4d	92.27	4.743	SMM	SMMM	4b,4c and SOC
4e	91.80	4.725	SMM	SMMS	4e and SOC
4f	95.29	4.626	SMS	SMS	SOC

M=~(CH_2O)~, S=SOC

The soluble polymer was isolated from 5 and 10 mole % SOC feed copolymerizations by extracting the products with acetone. The copolymers were found to contain 64 and 68 mole % SOC, respectively. A 500 MHz ^{1}H NMR spectrum of the 68 mole % SOC copolymer is shown in Figure III-C-10. The spectrum shows the same peaks seen in the acetal rich TOX-SOC copolymer (Figure III-C-7) with the large acetal singlet at 4.85 ppm replaced by a series of 6 resonances between 4.6 and 4.9 ppm arising from oxymethylene units of different sequence lengths. The peak assignments are listed on Table 3 along with long range correlations that should be observed by an HMBC. Figure III-C-11 shows the HMBC spectrum of the soluble copolymer oxymethylene region. Of the expected twelve correlations, ten are observed. Since the experiment can only confirm long range couplings between nuclei, the fact that two are not observed is presumably because $J_{^{13}C-^{1}H}$ involved is too small due to bond angles.

Pentad sequences were used to calculate average M unit sequence lengths of 2.4 and 2.9 for the 5 and 10 mole % samples, respectively. The S unit sequence lengths for the same samples were determined from the SS and SM dyads to be 7.6 and 6.9 units respectively.

Further evidence for the structure of the *insoluble* acetal rich copolymer fraction can be obtained through analysis of the HMBC cross peaks found in the *soluble* SOC rich copolymer spectra. Figure III-C-12 shows the full HMBC spectrum of the soluble copolymer. Highlighted in the spectrum is the correlation

to the carbonate carbon which is only observed via coupling to the protons on the methylenes numbered 1 and 1′. This correlation is not observed in the HMQC spectrum which shows single bond J_{C-H} coupling. To assign the remainder of the spectrum,the HMBC cross peaks have been superimposed on the HMQC spectrum shown in Figure III-C-13. Starting at the acetal unit, which is labeled 4d,4e,4f from the assignment explained previously, long range correlations can be made from 4d, 4e to 3′a and 4f to 3′b. These M to SOC connections prove that the product is in fact a copolymer. Correlations can also be made from 3′b to 1′ and 1′ to 2′. The methylenes from the SOC-SOC linkage can be assigned based on the following correlations: 1 to 3b and 2a indicates that these methylenes are in series; 3a and 3b to themselves, shows that the methylenes are symmetric about the ether bond; 3a to 2a and 3b to 2b shows that these methylenes are in series. Using the correlations above, the assignments in Figure III-C-14 have been made. The fact that two resonances are found for 3a,b and 2a,b may be due to shielding differences from the carbonate between conformers.

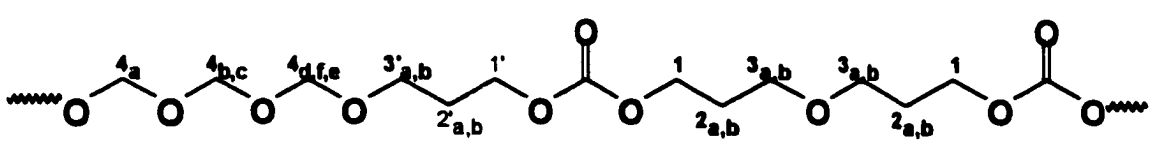

Figure III-C-14. Structure for TOX-SOC copolymer. Subscripts indicate different microstructures which are not shown.

CONCLUSIONS

TGA data (Table 2) indicate a significant stabilizing effect by SOC on polyacetal. Even at molar incorporations of 1% SOC, weight loss began for the copolymer at a temperature ~30°C higher than that in the case for TOX-DOL copolymer with a 2 mole % DOL incorporation.The stabilization effect increases with increased SOC incorporation. The degree of stabilization is however limited by the amount of SOC that can be incorporated into the insoluble copolymer. The percent crystallinity shows no trend across the available incorporation range and only varies by 8% from the lowest to highest value in the melt-crystallized samples. The T_m's as estimated by the DSC indicate a decreasing trend in copolymer melting point with increasing SOC incorporation as expected

References

[1] Takata, T., Endo, T. *Prog. Polym. Sci.*, **18**, 839, 1993

[2] Perrin, D., Armarego, W. *Purification of Laboratory Chemicals*, 3rd edn. Pergaman Press, Oxford and New York, 1988

[3] Endo, T., Okawara, M. *Synthesis*, **1984**, 837.

[4] Bax, A., Subramanian, S. *J. Magn. Reson.*, **1986**, 67, 565

[5] Bax, A., Summers, M. F. *J. Am. Chem. Soc.*, **1986**, 108, 2093

[6] Bax, *op. cit.*, 565

[7] Bax, *op. cit*, 2093

[8] Inoue, M. *J. Polym. Sci. A-1*, **1963**, 2697.

[9] Sakai, S., Kobayashi, Y., Ishii, Y. *J. Org. Chem.*, **1971**, 36, 9, 1176.

[10] Sakai, S., Fujinami, T., Sakurai, S. *J. Poly. Sci., Polym. Lett. Ed.*, **1973**, 11, 631.

[11] Penczek, S., Szymanski, R. *Polym. J.*, **1980**, **12**, 617

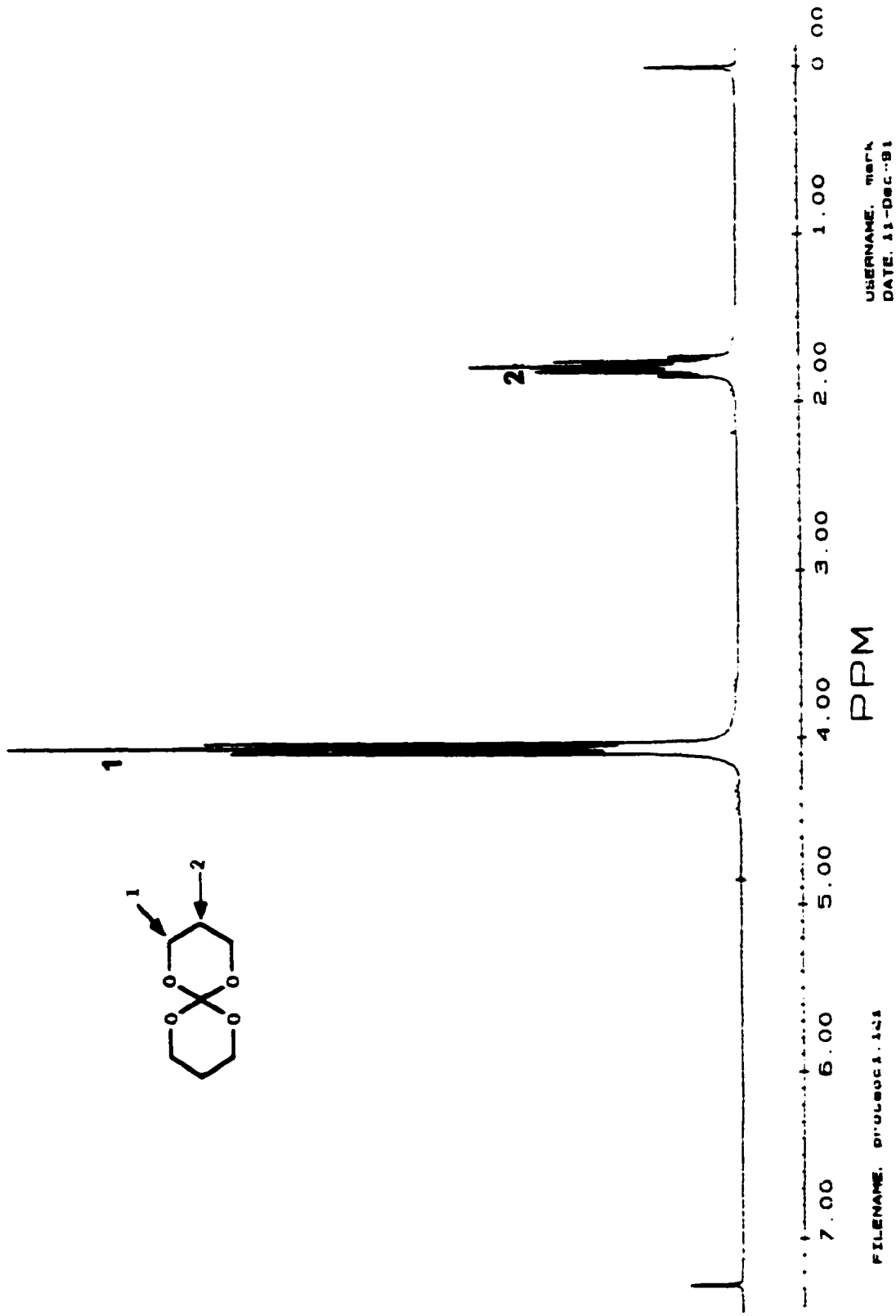

Figure III-C-1. 200 MHz ^{1}H NMR spectrum of 1,5,7,11-Tetraoxaspiro[5,5] Undecane in D-Chloroform.

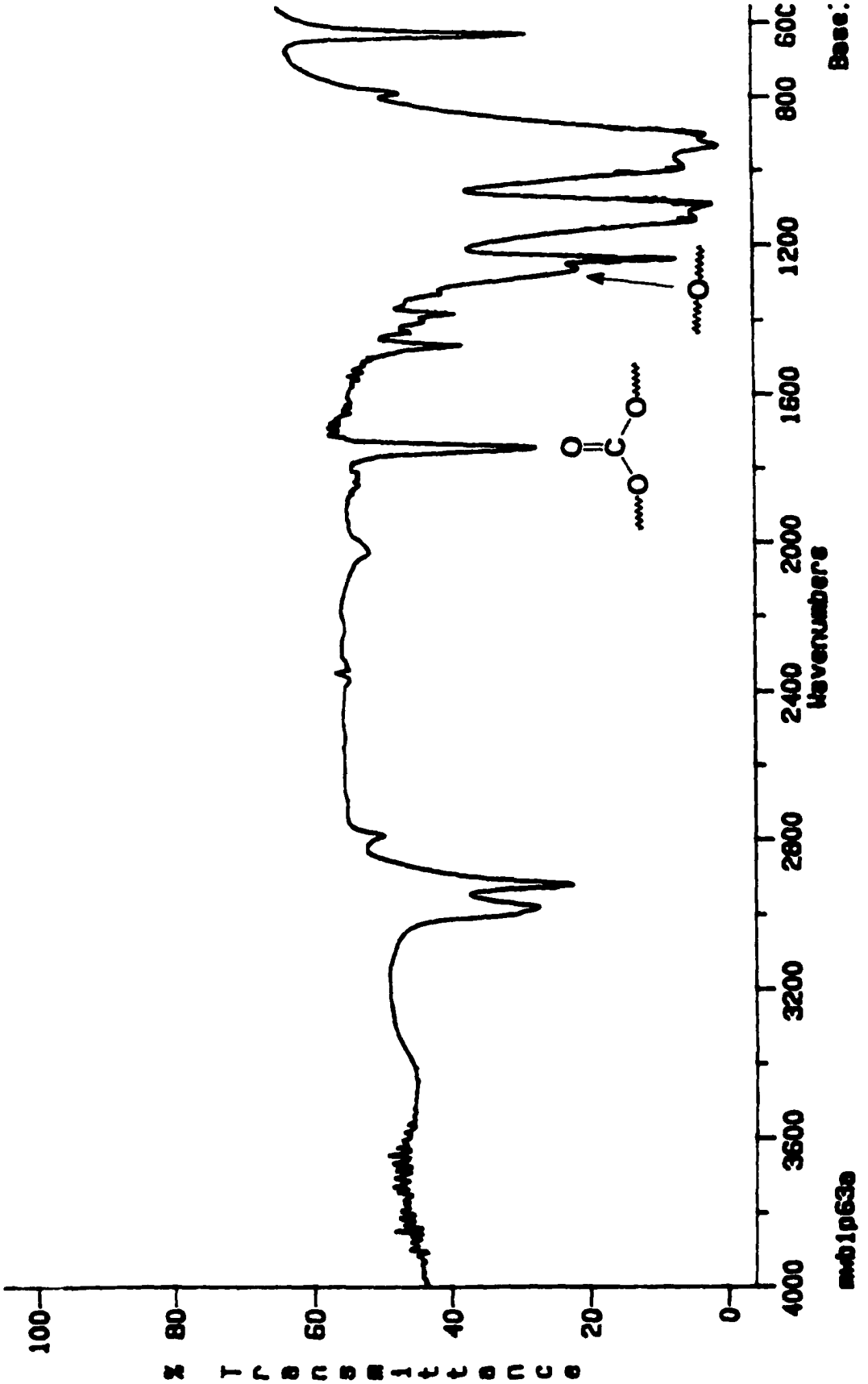

Figure III-C-3. Infrared Spectrum of TOX-SOC copolymer.

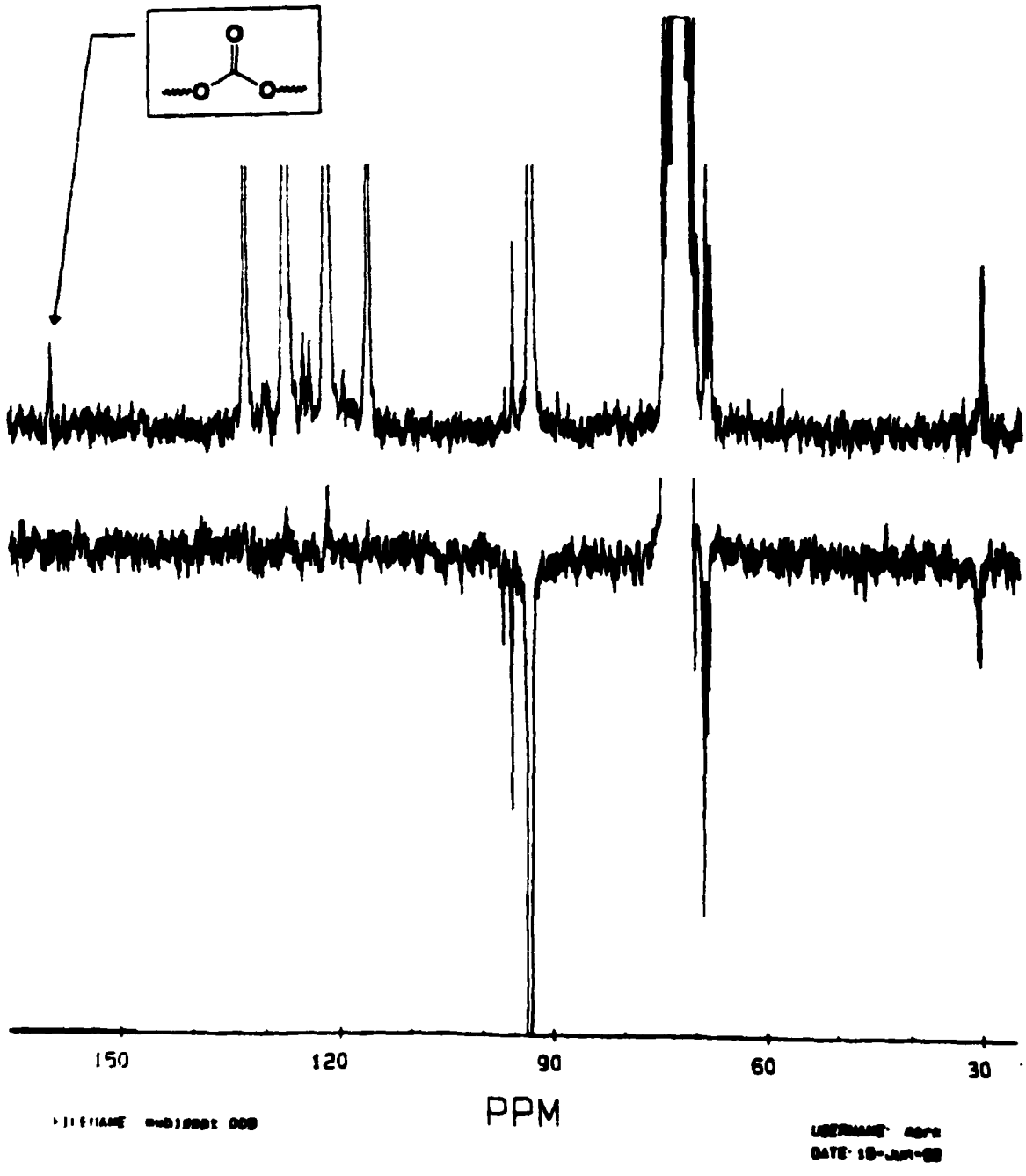

Figure III-C-4. TOX-SOC copolymer dissolved in HFIP. (TOP) 50 MHz ^{13}C NMR spectrum (bottom) 50 MHz ^{13}C DEPT spectrum.

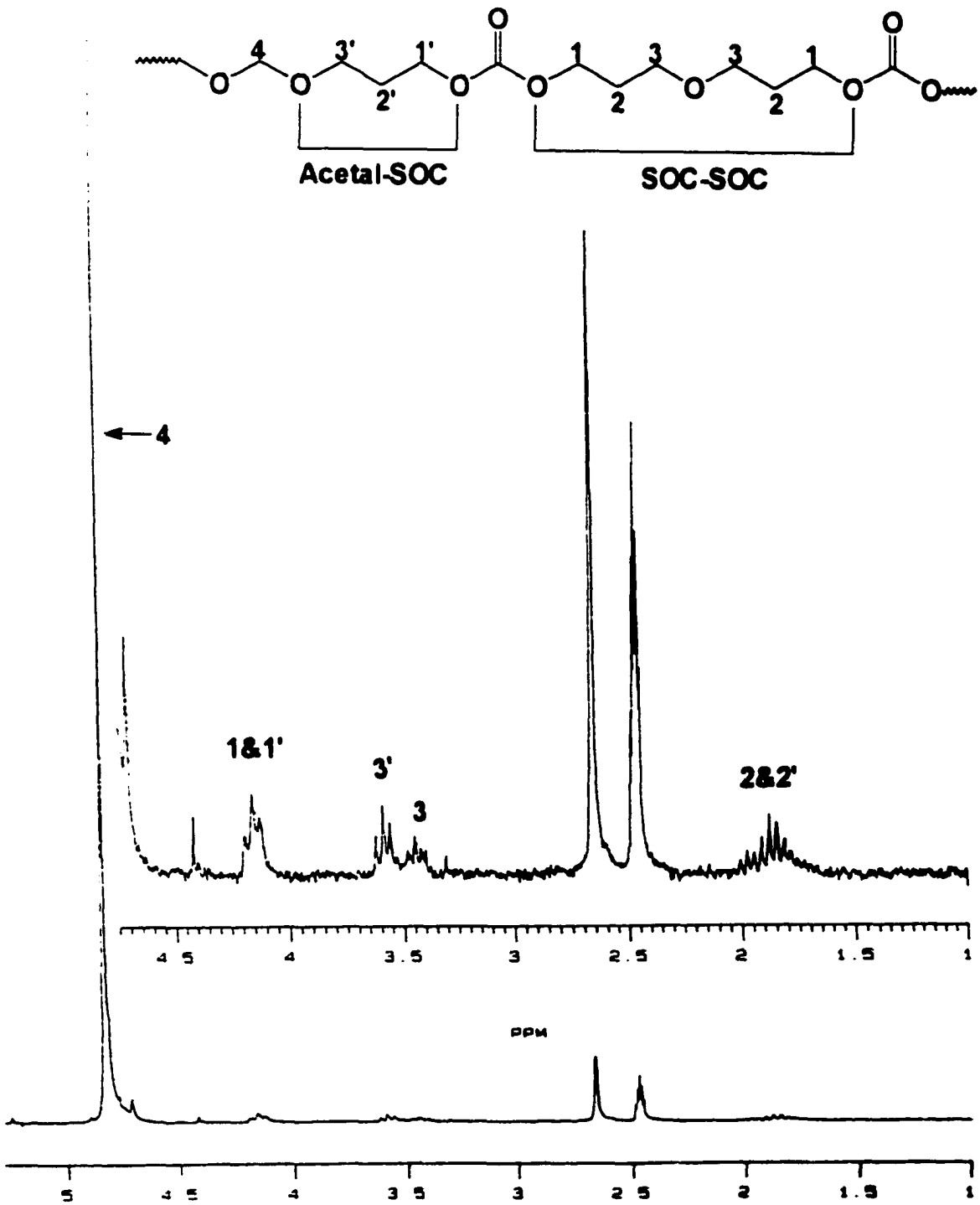

Figure III-C-5. 200 MHz ^{1}H NMR spectrum of acetal rich TOX-SOC copolymer acquired in DMSO at 120°C.

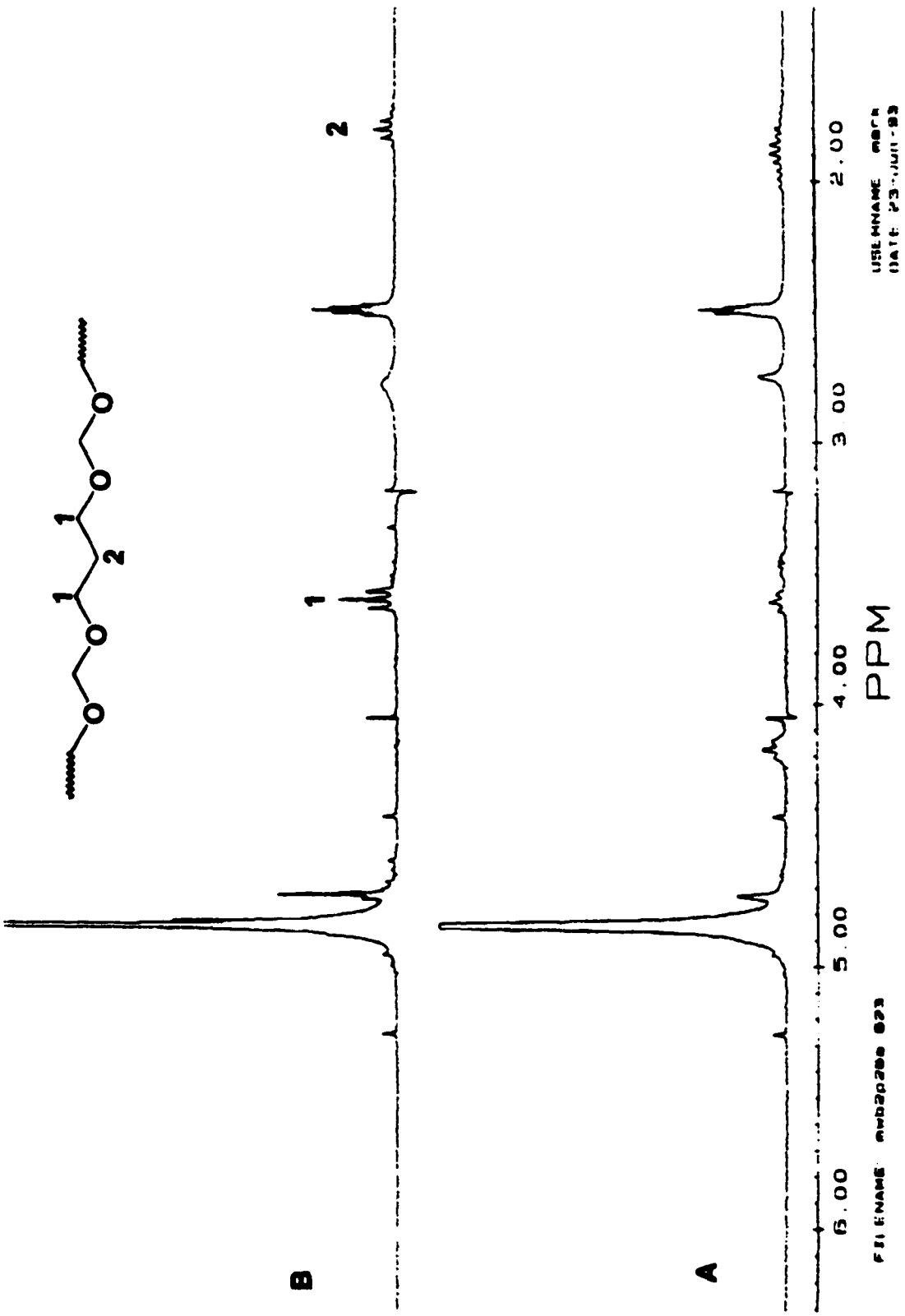

Figure III-C-6. 200 MHz ^{1}H NMR spectra acquired in DMSO at 120°C. a) TOX-SOC copolymer b) TOX-1,3-Dioxane copolymer.

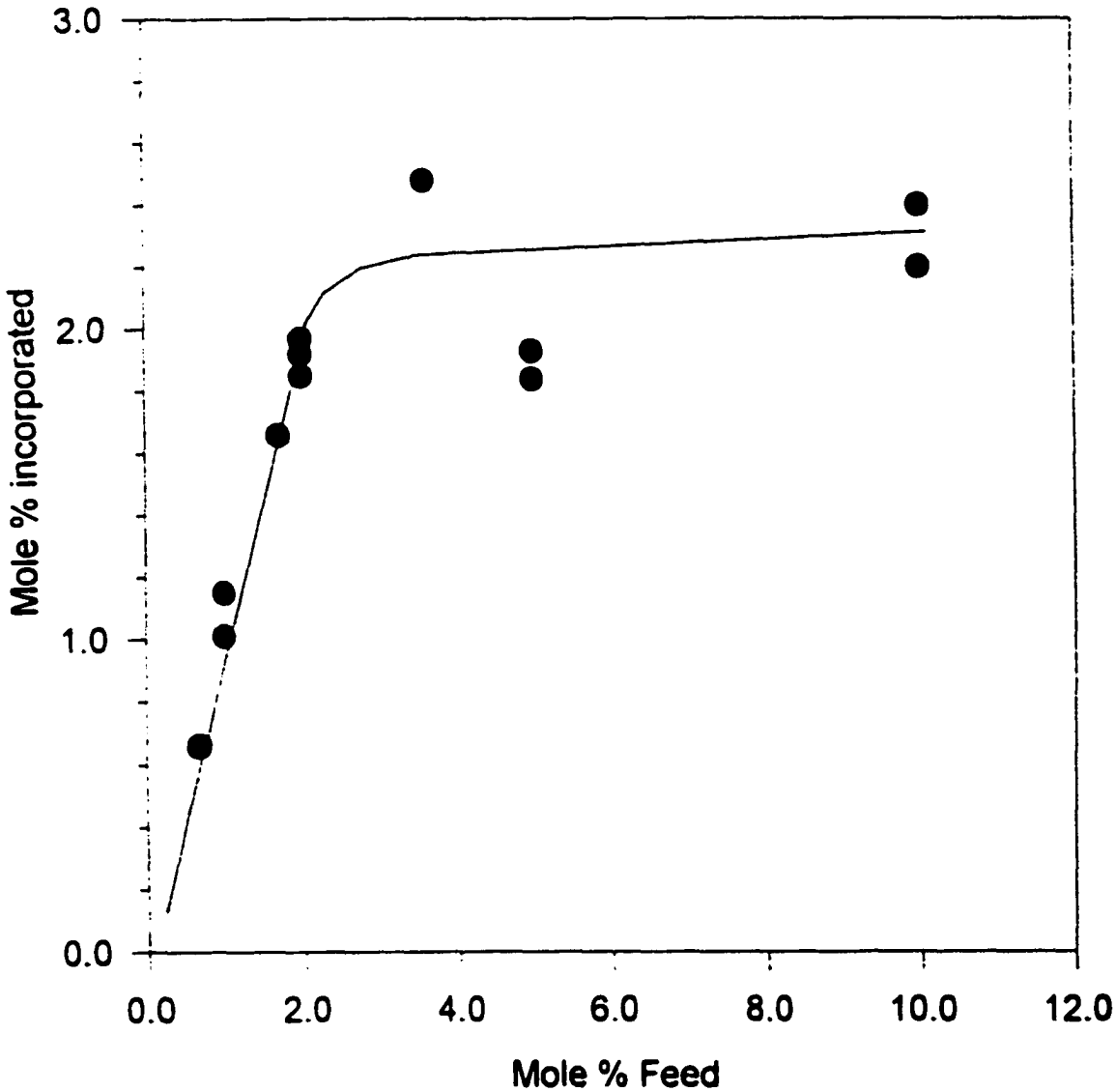

Figure III-C-8. SOC feed vs. incorporation in the acetal rich fraction of copolymer product.

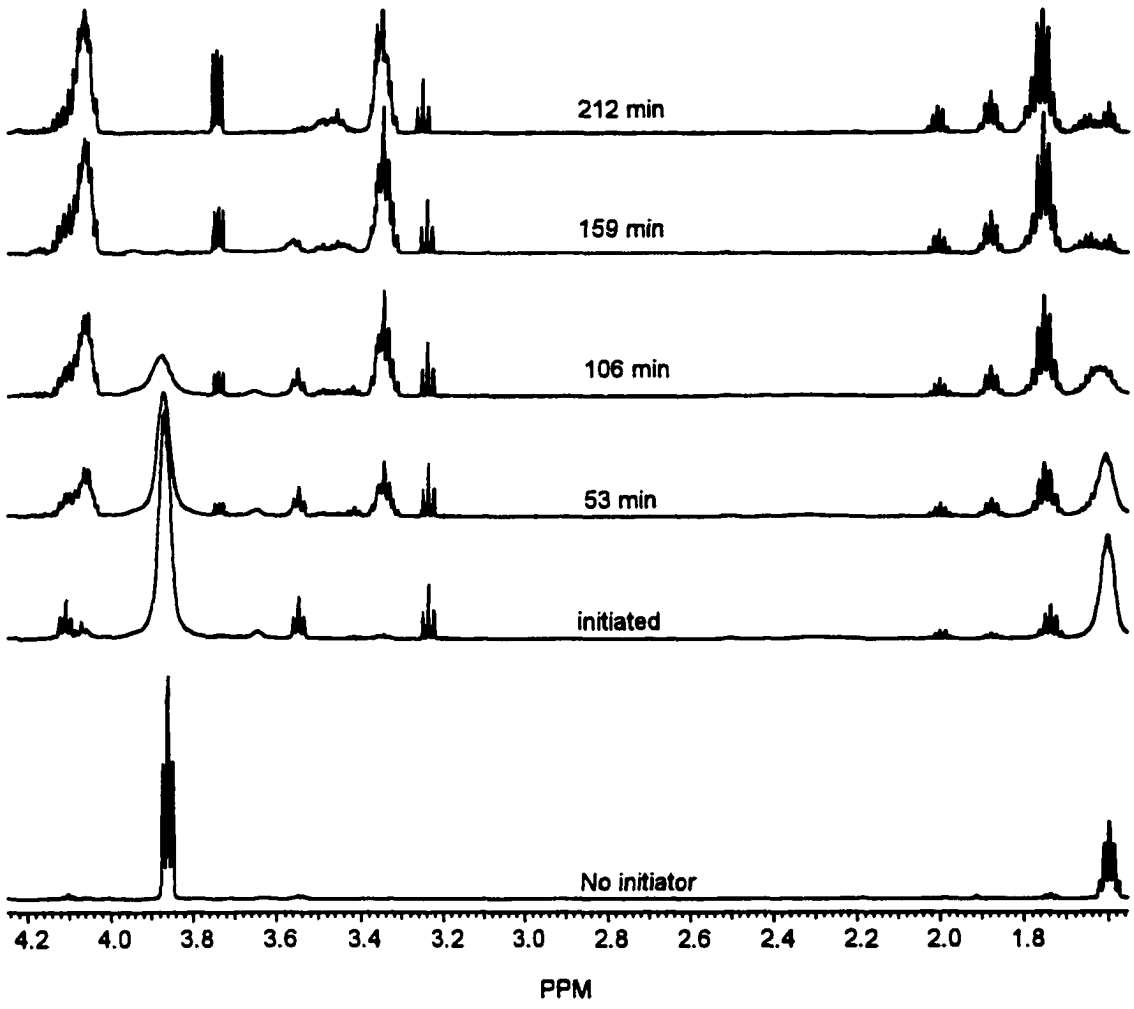

Figure III-C-9. 500 MHz ^{1}H NMR time series of TOX-SOC copolymerization at 40 °C, 4.0 M in chloroform-d, 20:1 mole ratio TOX to SOC, initiated by 3000 ppm BF_3OBu_2. Monomer spectrum (bottom) is displayed at 25% of its relative intensity

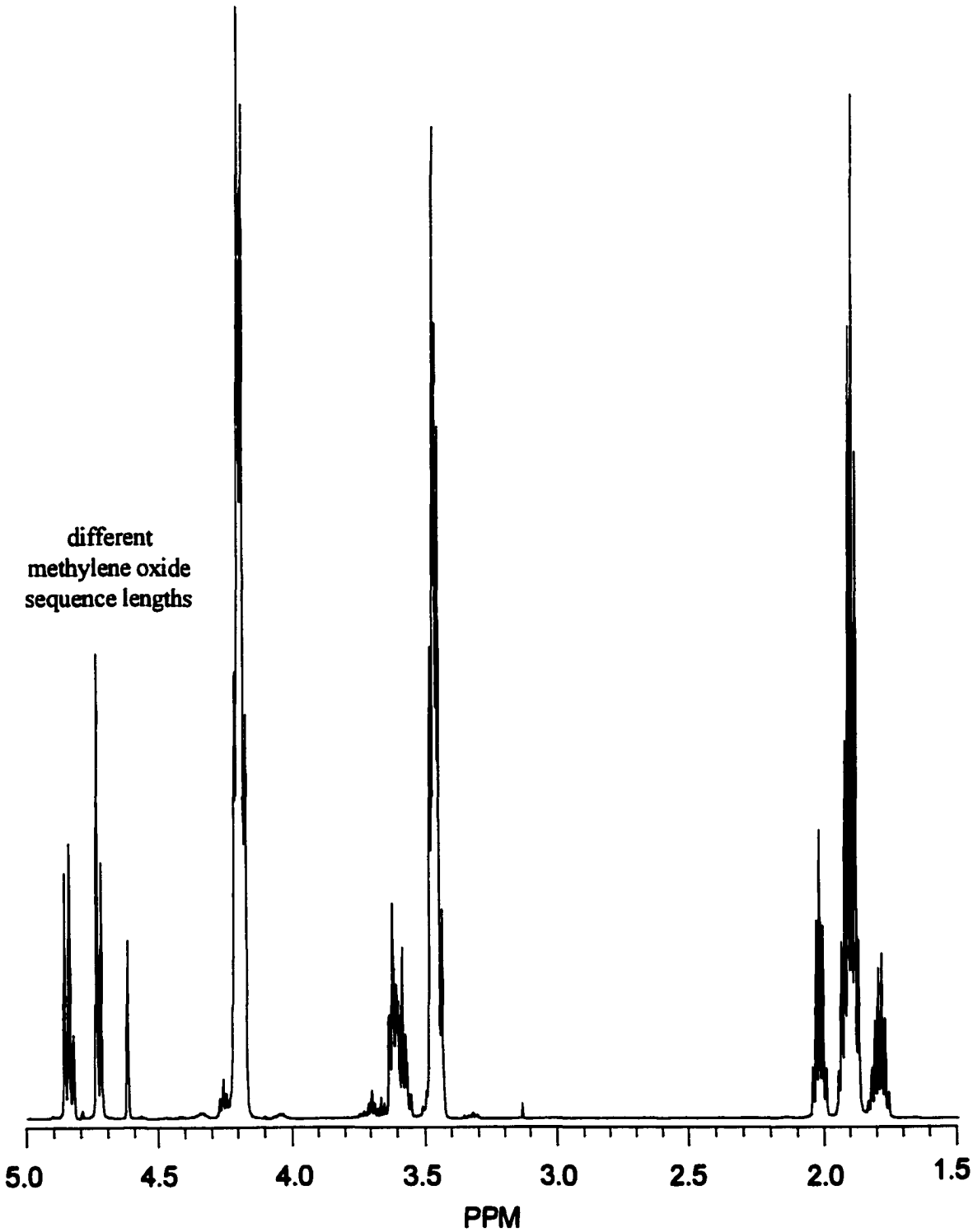

Figure III-C-10. 500 MHz ^{1}H NMR spectrum of soluble copolymer extracted after copolymerization

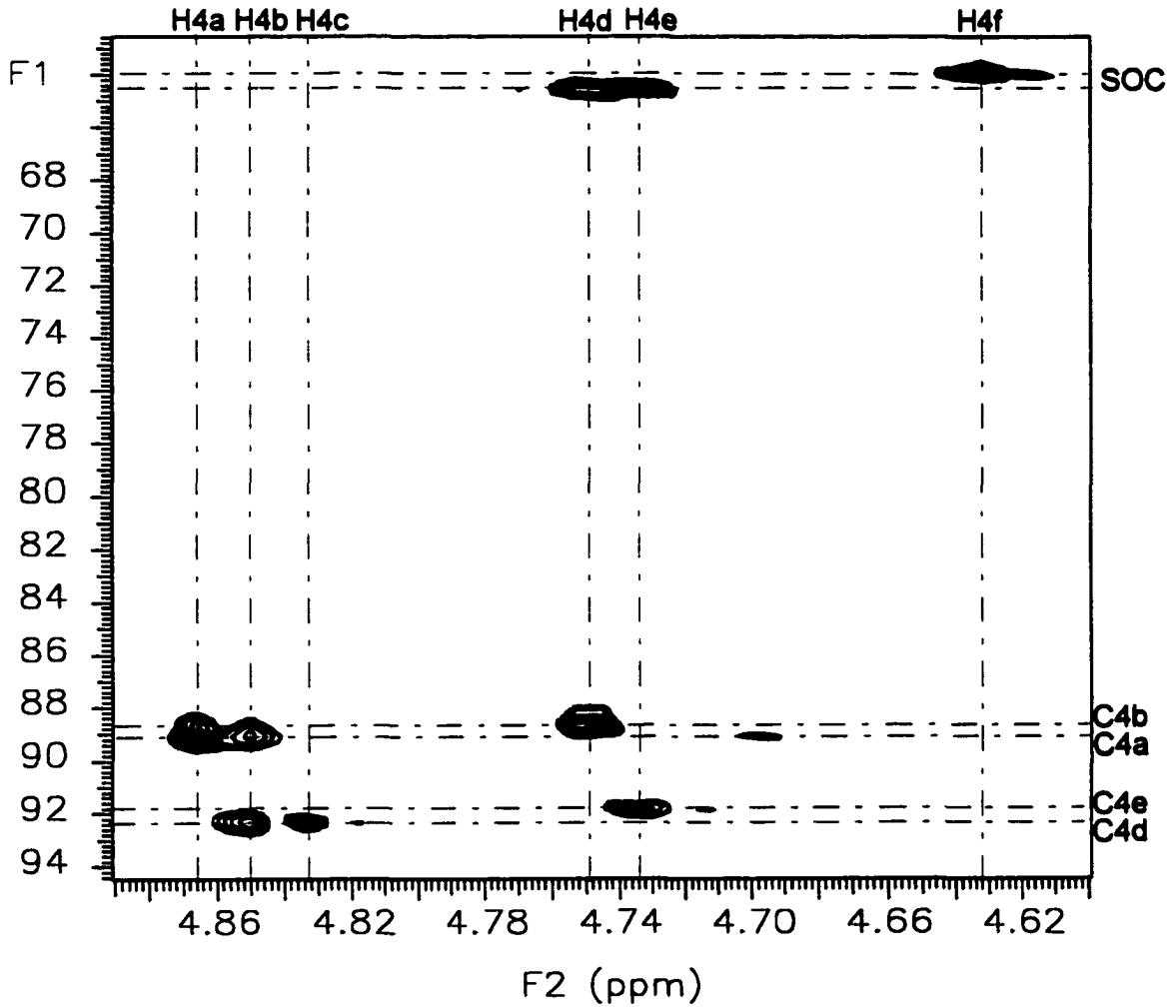

Figure III-C-11. 500 MHz HMBC spectrum of the oxymethylene region of TOX-SOC soluble copolymer, containing 68 mole % SOC. The copolymer was dissolved in chloroform-d and the spectrum was acquired at 30°C.

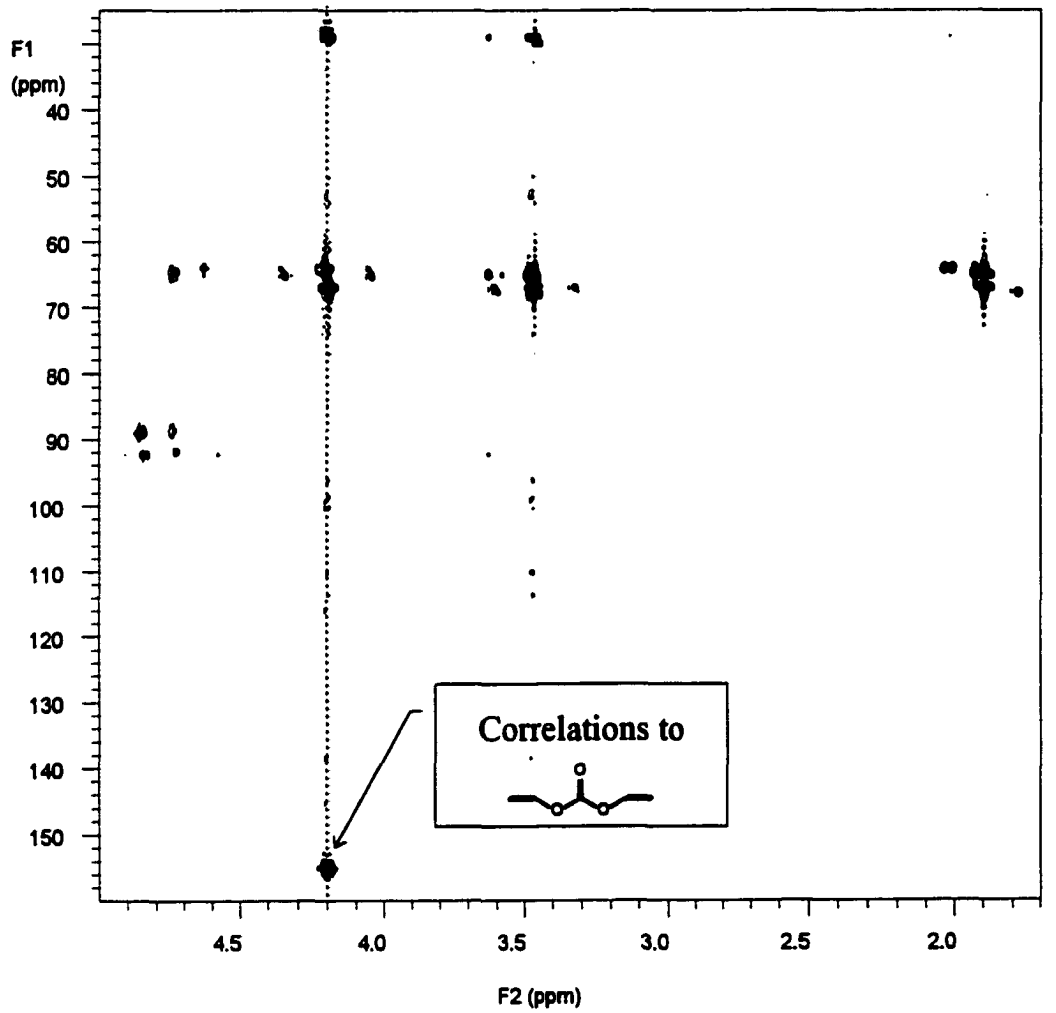

Figure III-C-12 . 500 MHz HMBC spectrum of soluble TOX-SOC copolymer at 30°C. The copolymer was dissolved in chloroform-d.

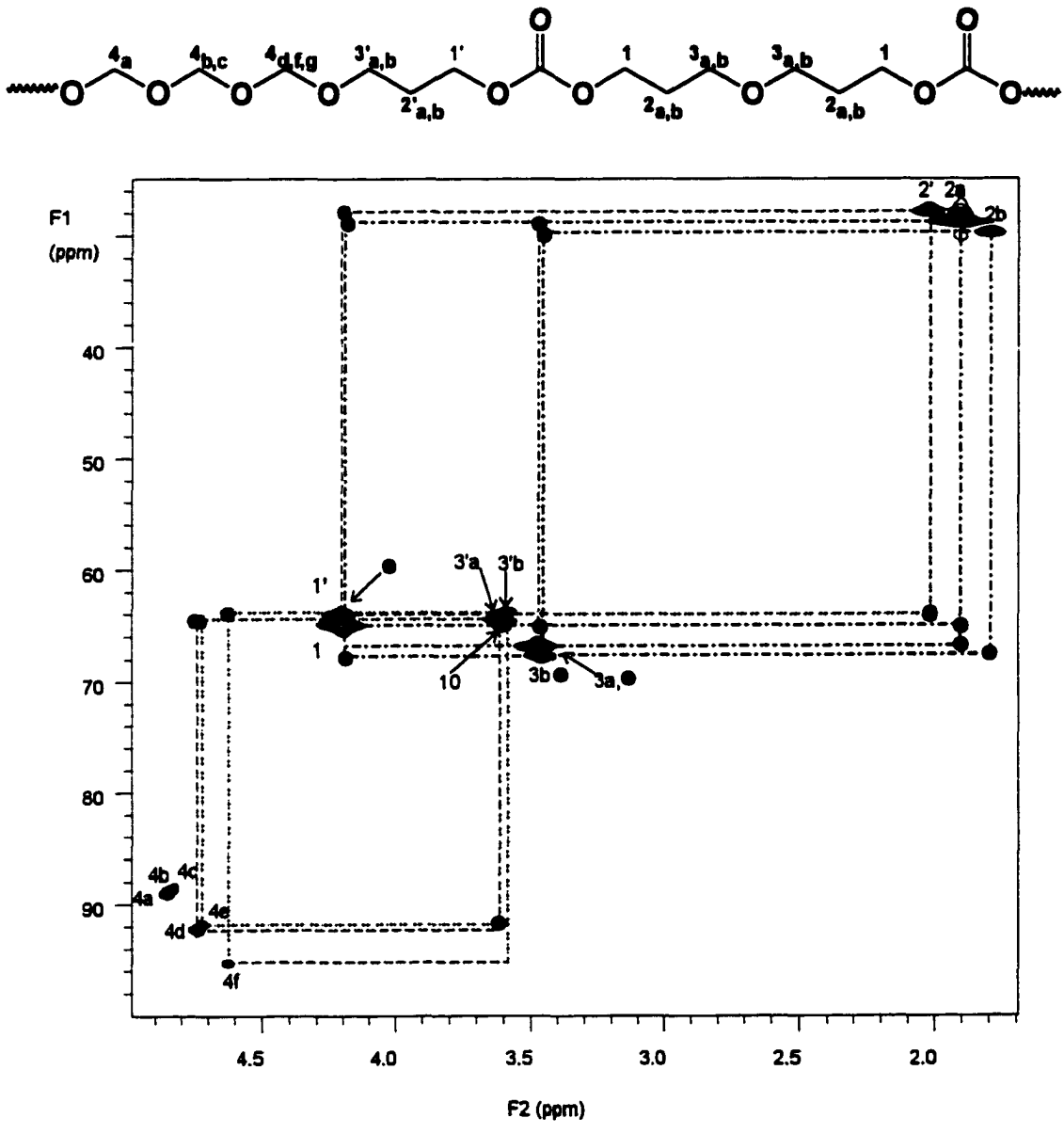

Figure III-C-13. HMQC spectrum of soluble TOX-SOC copolymer. ●'s are located where correlations are found in the HMBC spectrum. Peaks 3a and 3b have cross peaks to themselves and there is a cross peak very near peak 1'.

IV Concluding Remarks

The goal of this investigation was to develop a full understanding of the chemical processes that occur during the copolymerization of trioxane and dioxolane. Although this goal has not been completely achieved, progress has been made toward this end.

The most important contribution made toward understanding the copolymerization was the clarification of the role that transacetalization plays during the "precloud period". The *in situ* NMR experiments demonstrated that DOL rich copolymer formed early in the copolymerization remains largely intact through the "precloud period" and is not redistributed by the transacetalization mechanism. By analyzing copolymer samples isolated at various points after the onset of clouding, it was shown that it is during the "postcloud-period" that the ethylene oxide units are redistributed to form an almost random copolymer. The *in situ* NMR experiments using ^{13}C enriched DOL also helped to shed light on the "precloud period". They proved that there is a facile exchange of methylene oxide units throughout the system prior to the onset of polymerization.

In addition to the mechanistic information we also developed objective NMR assignments of the main chain sequence, endgroups, penultimate units and junction units present in the TOX-DOL copolymer. Only the inherently unstable hemiacetal endgroup could not be assigned. This project demonstrated the useful role that modern NMR can play in the field of polymer chemistry and provides a

useful approach that can be applied to other polymer systems.

The copoloymerization of SOC helps to clarify further the role that formaldehyde plays in the TOX-DOL copolymerization. In this system formaldehyde only begins to build up after all of the SOC is consumed. This inhibits TOX from polymerizing to any appreciable degree until all of the SOC is consumed, showing that TOX polymerization is dependent on formaldehyde reaching its equilibrium concentration. The amorphous nature of the SOC copolymer units seems to greatly reduce the effect of transacetalization during the this copolymerization

BIBLIOGRAPHY

I Background Survey

1 Masamoto, J., Iwaisako, T., Yoshida, K., Matsuzaki, K., Kagawa, K., Nagahara, H. *Makromol. Chem., Macromol. Symp.*, 1991, 42/43, 409

2 Butlerov, A.M. *Ann.* 1859, **3**, 242

3 Staudinger, H. *Die Hochmolecularen Organischen Verbingen*, Springer: Berlin, 1932

4 Kern, W., Cherdron, H., Jaacks, V. Angew. Chem., 1961, **73**, 177

5 MacDonald, R. N. (to E. I. du Pont de Nemours & Co. Inc.) U. S. Patent 3 027 352, March 27, 1956

6 Walling, C.; Brown, F.; Bartz, K. (to Celanese Corp.) U.S. Patent 3 027 352, March 27, 1962

7 Dolce, T.; McAndrew, F. "Acetal Copolymers, A Historical Perspective," in High Performance Polymers : Origins and Development, G. Kirshenbaum and R. Seymor, Eds. ; American Chemical Society : Washington, D.C., 1986, p 115.

8 Weissermel, K., Fisher, E., Gutweiler, K., *Kunstoffe*, 1964, **54**, 410

9 Weissermel, K., Fisher, E., Gutweiler, K., Hermann, H. D., Cherdron, H., *Angew. Chem. Int. Ed.*, 1967, **6**, 526

10 Chen, C.S.H.; DiEdwardo, *A. Adv. Chem. Ser.*, 1969, **91**, 359.

11. Chen, C.S.H., DiEdwardo, *J. Macromol. Sci. Chem.*, 1970, **4**, 349.

12. Weissermel, K., Fisher, E., Gutweiler, K., Hermann, H. D., Cherdron, H., *Angew. Chem. Int. Ed.*, 1967, **6**, 526

13. Collins, G.L.; Greene, R.K.; Berardinelli, F.M.; Ray, W.H. *J. Polym. Sci. Polym. Chem. Ed.*, 1981, **17**, 667.

14. Masamoto, J., Iwaisako, T., Yoshida, K., Matsuzaki, K., Kagawa, K., Nagahara, H., *Makromolek. Chem., Macromolec. Sym.*, 1991, **42/43**, 409

15. Collins, G.L.; Greene, R.K.; Berardinelli, F.M.; Ray, W.H. *J. Polym. Sci. Polym. Chem. Ed.*, 1981, **17**. 667.

16. Price, M. B., Mcandrew, F. B., *J. Macromolec. Sci., A-I,* 1967, **2**, 231

17. Miki, T., Higashimura, T., Hayashi, K., Okamura, S., *J. Polym. Sci., Polym. Lett.*, 1967, **5**, 65

18. Jaacks, *V., Adv. Chem. Ser.*, 1969, **91**, 371

19. Mengoli, G., Furlanetto, F. *Makromolek. Chem.*, 1975, **176**, 143

20. Lu, N., Collins, G. L., Yang, N. L., *Macromol. Chem., Macromol. Symp.*, 1991, **42/43**, 425

21. Wessermel, K., Fisher, E., Gutweiler, K., *Kunstoffe*, 1964, **54**, 410

22. Jaacks, *op. cit.*,

II Thesis Statement and Outline

1 Chen, C. S. H., Di Edwardo, A. *Adv. in Chem.*, 1969, **91**, 359

2 Lu, N., Collins, G. L., Yang, N. L. *Macromol. Chem., Macromol. Symp.*, 1991, **42/43**, 425

III Results and Discussion

III-A

1 Yamahita, Y., Asakura, T., Okada, M., Ito, K. *Makromol. Chem.*, 1969, **129**, 1

2. Fleischer, D., Schulz, R. C. *Makromol. Chem.*, 1975, **176**, 677

3. Beshah, K. *Makromol. Chem.*, 1993, **194**, 3311

4. Beshah, K. *Macromol. Symp.*, 1994, **86**, 34

5. Rinaldi, P. L., Keifer, P. A. *J. Magn. Reson.*, 1994, **108**, 259

6. Hurd, R. E., John, B. K. *J. Magn. Reson.*, 1991, **91**, 648

7. Rinaldi, *op. cit.*,

8. Lerner, L., Bax, A. *J. Magn. Reson.*, 1986, **69**, 375

9. States, D. J., Haberkorn, R. A., Ruben, D. J. *J. Magn. Reson.*, 1982, **48**, 286

[10.] Griesinger, C., Otting, G., Wüthrich, K., Ernst, R. R. *J. Am. Chem. Soc.* **1988, 110,** 7870

[11.] Jaacks, V., Frank, H., Grünberger, E., Kern, W. *Makromol. Chem.* **1968, 115,** 290

III-B

[1] Jaacks, V. *Adv. Chem. Ser.*, 1969, **91**, 371

[2] Yamashita, Y., Asakura, T., Okada, M., Ito, K. *Makromol. Chemie*, 1969, **129**, 1

[3] Dale, J., Ekeland, T., Krane, J. *J. Am. Chem. Soc.*, 1972, **94**, 1389

III-C

[1] Takata, T., Endo, T. *Prog. Polym. Sci.*, **18**, 839, 1993

[2.] Perrin, D., Armarego, W. *Purification of Laboratory Chemicals*, 3rd edn. Pergaman Press, Oxford and New York, 1988

[3.] Endo, T., Okawara, M. *Synthesis*, **1984**, 837.

[4.] Bax, A., Subramanian, S. *J. Magn. Reson.*, **1986**, 67, 565

[5.] Bax, A., Summers, M. F. *J. Am. Chem. Soc.*, **1986**, 108, 2093

[6.] Bax, *op. cit.*, 565

[7.] Bax, *op. cit*, 2093

[8.] Inoue, M. *J. Polym. Sci. A-1*, **1963**, 2697.

[9.] Sakai, S., Kobayashi, Y., Ishii, Y. *J. Org. Chem.*, **1971**, 36, 9, 1176.

[10.] Sakai, S., Fujinami, T., Sakurai, S. *J. Poly. Sci., Polym. Lett. Ed.*, **1973**, 11, 631.

[11.] Penczek, S., Szymanski, R. *Polym. J.*, **1980, 12**, 617